Synergistic effects of anti-V3 and CD4bs antibodies against HIV-1

Recent studies on functional trimers of envelopes suggest that exposure of V3-epitope and coreceptor binding sites including the CD4i epitope occurs following the interaction of gp120 with CD4 (Kwong et al., 2002, 1998; Liu et al., 2008; Mbah et al., 2001). In fact, sCD4-mediated enhancement was observed in the V3 and CD4i MAbs (Fig. 2), as has been previously reported (Lusso et al., 2005; Thali et al., 1993; Wu et al., 2008). We then tested whether antibodies to CD4bs have the capacity to alter the envelope conformation and induce some critical epitopes accessible for the antibodies of other specificities. We first tested the binding activity of MAbs in the presence or absence of the CD4bs MAb 0.5δ by ELISA (Fig. 5). Marked enhancement of binding of 0.5γ was observed in the presence of 0.5δ. The enhancement was also observed for the other V3 antibody 3E4, although the effect was much higher in 0.5γ than in 3E4. In contrast, suppression in the binding of 0.5δ itself and CD4i MAb 4C11 was observed in the presence of 0.5δ. This suggests that the 0.5δ epitope may overlap with that of 4C11, or that the binding of either MAb may interfere with the other sterically.

Then, we tested the effect of MAbs combinations, such as 0.5γ (V3) and 0.5δ (CD4bs), 1D9 (V3) and 49G2 (CD4i), and 16G6 (V3) and 17G2 (V3) over neutralization. The combinations of MAbs showed an additive effect in most of cases, while the combination of 0.5γ and 0.5δ showed a synergistic effect in the neutralizing activity of HIV-1$_{JR-FL}$ (Fig. 6). The combination of these MAbs was shown to be more effective than either MAb alone and the synergy of neutralizing activity observed for the combination of 0.5γ and

0.5δ was up to 25% (Supplementary Table 3). This result suggests that these antibodies, besides their complementarity, can act synergistically. This phenomenon of synergism and complementarity may play an important role "in vivo" for suppressing viruses in a patient.

ADCC activities of the MAbs

It has been reported that antibodies contribute to protection by its effector-mediated functions such as ADCC (Haynes et al., 2012a; Liao et al., 2013; Xiao et al., 2010). Then, we determined the ADCC activities of MAbs from patient KTS376. First, we analyzed cells coated with gp120 from SF2 and cells infected with BaL and YU2 (Fig. 7, Supplementary Fig. 3). Significant ADCC activity was observed in most of the MAbs from the three groups. The CD4i MAb 916B2 showed neutralizing activity against BaL, but did not show any statistically significant ADCC activity against BaL. The 916B2 epitope may require the CD4 binding to Env, as reported previously (Veillette et al., 2014). ADCC activity of MAbs from patient KTS376 was also evaluated against cells infected with five T/F virus strains (Fig. 8, Supplementary Fig. 4). ADCC activity for the T/F viruses was relatively weak compared with the response observed for gp120, BaL and YU2. THRO was sensitive to all the MAbs tested, while ADCC activity against CH106 was statistically significant in CD4bs MAb 49G2. Interestingly, the V3 MAbs acted complementarily against CH040 and REJO. ADCC activity against CH040 was observed in MAbs, 0.5γ and 16G6, and the other V3 MAbs were effective against REJO. Despite the fact that no neutralizing activity was observed for THRO, all the MAbs showed
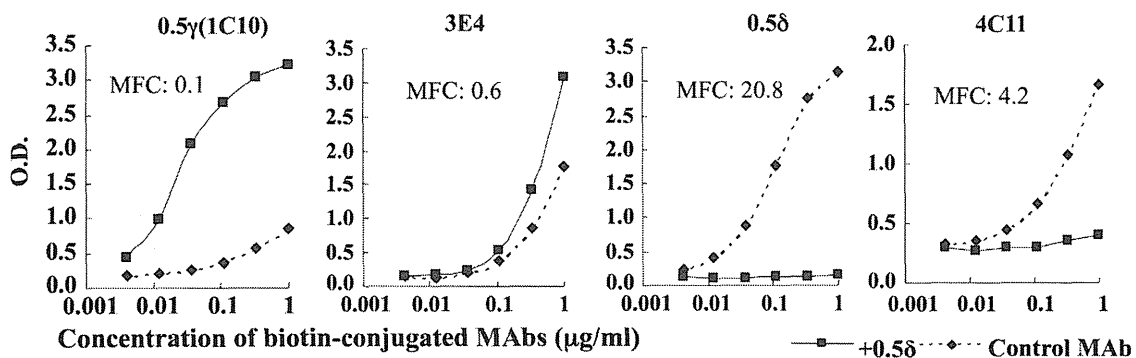

Fig. 5. **Effect of CD4bs MAb 0.5δ on reactivity of other MAbs.** Reactivity of MAbs was analyzed by ELISA for biotin conjugated antibody alone (dotted line) or in combination with 0.5δ (solid line). Marked enhancement of reactivity in the presence of 0.5δ was observed in the MAb to V3 0.5γ. Another anti-V3 MAb 3E4 showed only a slight enhancement by 0.5δ, and abrogation of reactivity was evident for 0.5δ and 4C11. Maximum fold change (MFC) was calculated as follows: O.D 0.5δpositive/ O.D. 0.5δ negative.

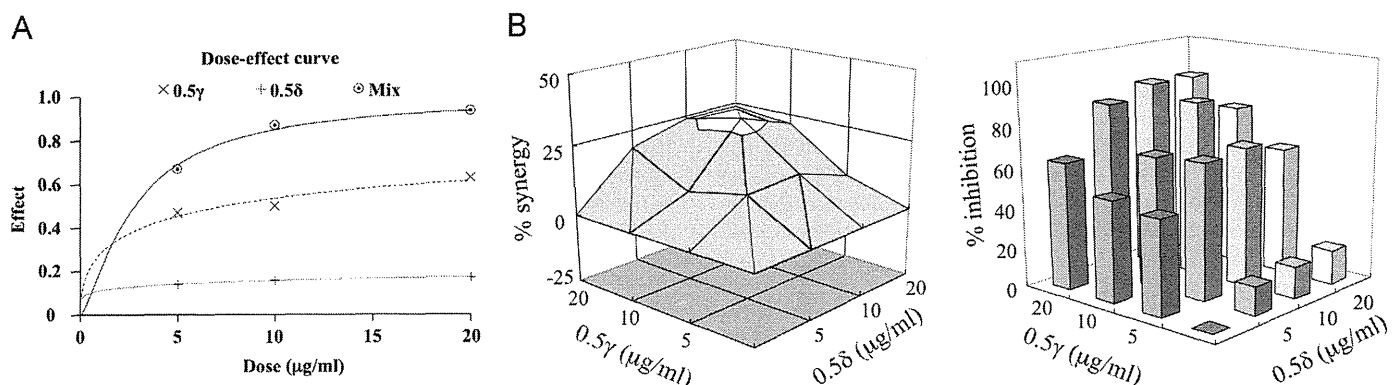Fig. 6. **Synergistic neutralizing activity of the anti-V3 MAb 0.5γ and the CD4bs MAb 0.5δ.** Neutralization activity of 0.5γ alone (X symbol), 0.5δ alone (+ symbol) and 1:1 combination of both MAbs (Circle and dot symbol) was evaluated and is shown as a dose-effect curve (A). The percentages of synergy (B) and viral inhibition (C) reached by combinations of 0.5γ and 0.5δ are shown. Neutralizing activity was analyzed against HIV-1$_{JR-FL}$. Synergy between 0.5γ and 0.5δ was calculated using the Chou–Talalay method and 3 dimensional analyses.
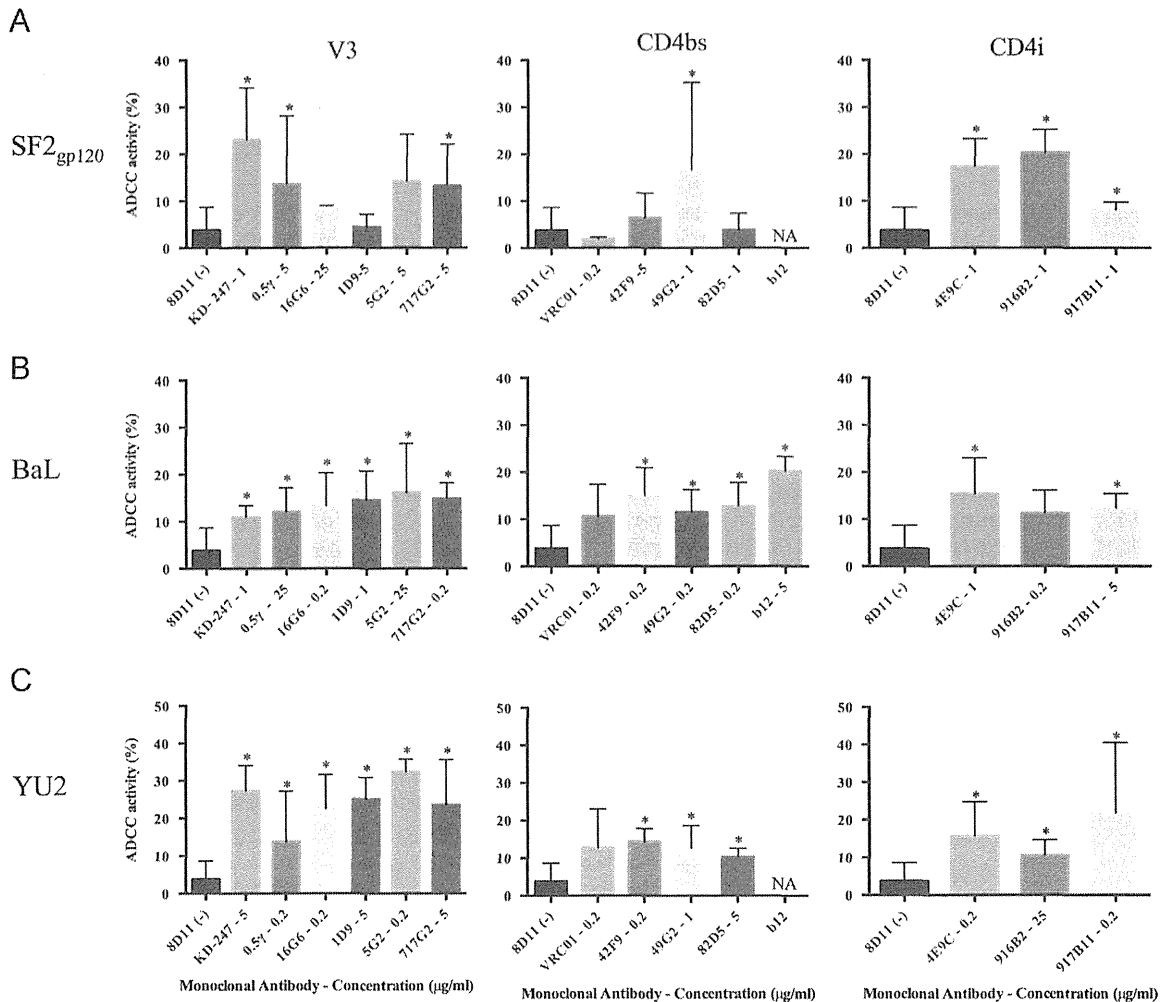
Fig. 7. ADCC activity of MAbs against CEM.NKr.CCR5 cells coated with SF2$_{gp120}$ (A), infected with BaL (B) and YU2 (C). ADCC activity was evaluated using CEM.NKr.CCR5 cells stained with CFSE and PKH-26 as target cells and PBMC (A and C) or NK-enriched PBMC (B) from healthy donors as effector cells. MAb concentration between 0.2 and 25 μg/ml was analyzed, and the maximum percentages of killing are shown for each MAb. Concentration of MAb (μg/ml) is indicated together with MAb name. Asterisks correspond to values statistically different from the negative control ($p < 0.05$) calculated with the Mann–Whitney U test.

significant ADCC activity against this virus. This indicates that ADCC activity is not correlated with neutralizing activity. However, CH106 was resistant to both neutralization and ADCC.

These results demonstrated that MAbs from a single donor presented ADCC activity against HIV-1 strains including T/F viruses. The coverage of a wide range of HIV-1 strains by ADCC supports the complementary character of these MAbs from a single patient, not only for the neutralizing activities, but also for the non-neutralizing activities.

Presence of KTS376-like antibodies in plasma samples

In order to determine the presence of antibodies with the specificity similar to the MAbs from patient KTS376, plasma samples from various patients were examined for the ability to block binding of 0.5γ, 3E4, 0.5δ and 4C11 (Fig. 9, Supplementary Fig. 5). Plasma samples from HIV-1-infected patients, which included progressors ($N=47$), slow progressors ($N=25$), long-term non-progressors, LTNP ($N=20$) and non-B-infected ($N=11$) patients, significantly suppressed the binding of CD4bs MAb 0.5δ and CD4i MAb 4C11. This is consistent with a previous observation that most of the patients have antibodies to CD4bs and CD4i (Binley et al., 2008; Dhillon et al., 2007; Gnanakaran et al., 2010; Moulard et al., 2002; Sather et al., 2009). The V3 MAbs, 0.5γ and 3E4, were not inhibited significantly by plasma samples from non-

B-infected patients, and this maybe due to the poor cross-subtype reactivity of the V3 MAbs (Fig. 3). Disease progression was associated with the low inhibition of MAbs, and the plasma samples from progressors inhibited the binding of MAbs less strongly than those from LTNP. Accordingly, the inhibition of 0.5γ, which was weakly inhibited by plasma samples compared with other MAbs, was not significant in progressors. However, considerably longer times of infection in the long-term non-progressor and the slow progressor groups may have contributed to affinity maturation of antibodies in these groups. This suggests that the presence of antibodies similar to those in patient KTS376 may contribute to the control of HIV-1 infection. On the other hand, KTS376-like antibodies were found in most of HIV-1-infected patients regardless of their disease status, suggesting that antibodies against V3, CD4bs and CD4i were induced in most HIV-1-infected patients similarly to patient KTS376.

Discussion

In the present study, we isolated 25 MAbs from a patient, KTS376, who had suppressed HIV-1 infection for more than 25 years without any treatment, and further analyzed these MAbs to clarify the mechanism to controlling HIV-1 infection. A wide coverage of viruses by a set of monoclonal antibodies from
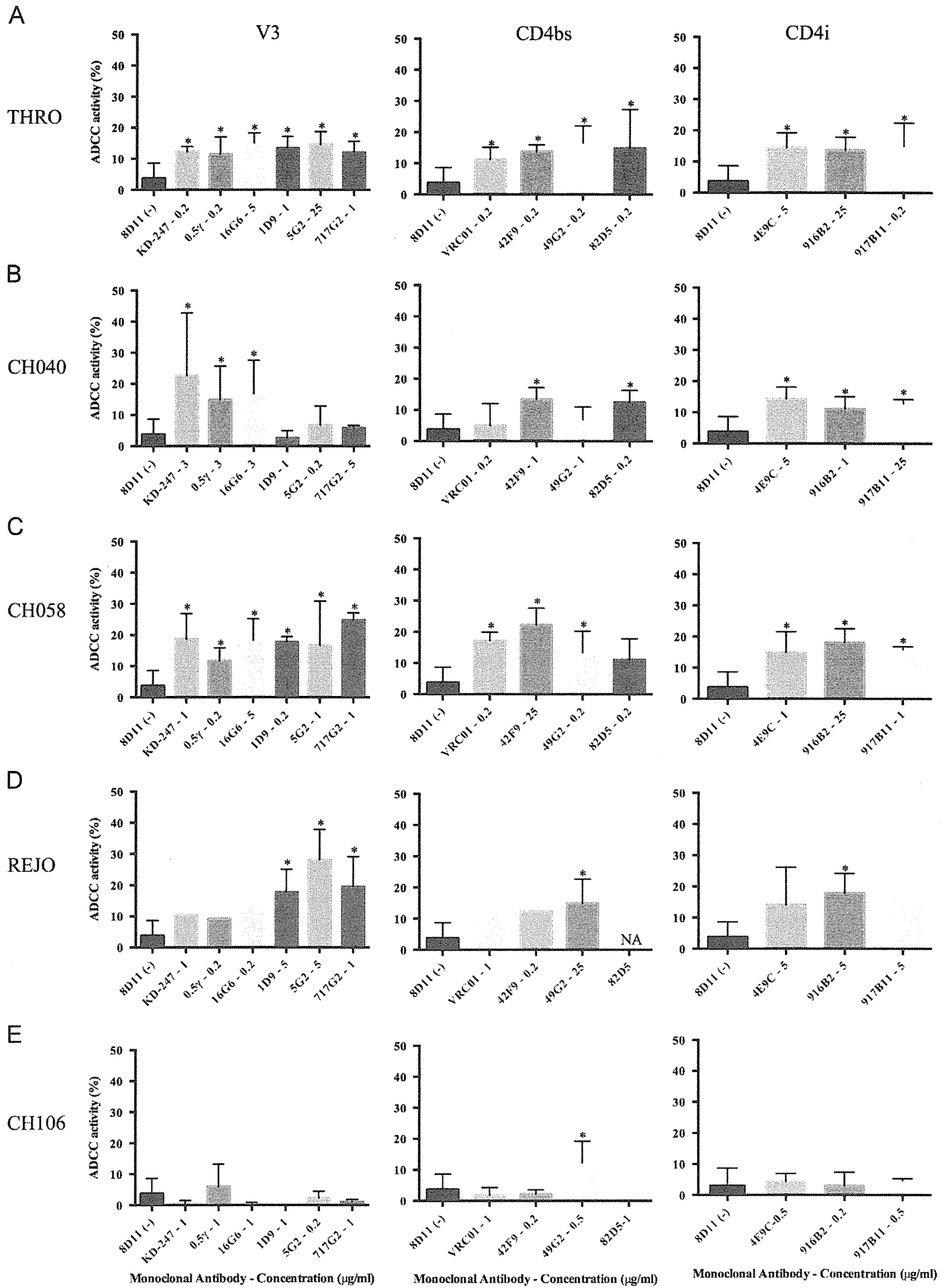
Fig. 8. ADCC activity of MAbs against CEM.NKr.CCR5 cells infected with T/F viruses, THRO (A), CH040 (B) CH058 (C) REJO (D) and CH106 (E). ADCC activity was evaluated using CEM.NKr.CCR5 cells stained with CFSE and PKH-26 as target cells and PBMC (C, D and E) or NK-enriched PBMC (A and B) from healthy donors as effector cells. MAb concentration between 0.2 and 25 µg/ml was analyzed, and the maximum percentages of killing are shown for each MAb. Concentration of MAb (µg/ml) is indicated together with MAb name. Asterisks correspond to values statistically different from the negative control ($p < 0.05$) calculated with the Mann–Whitney U test.
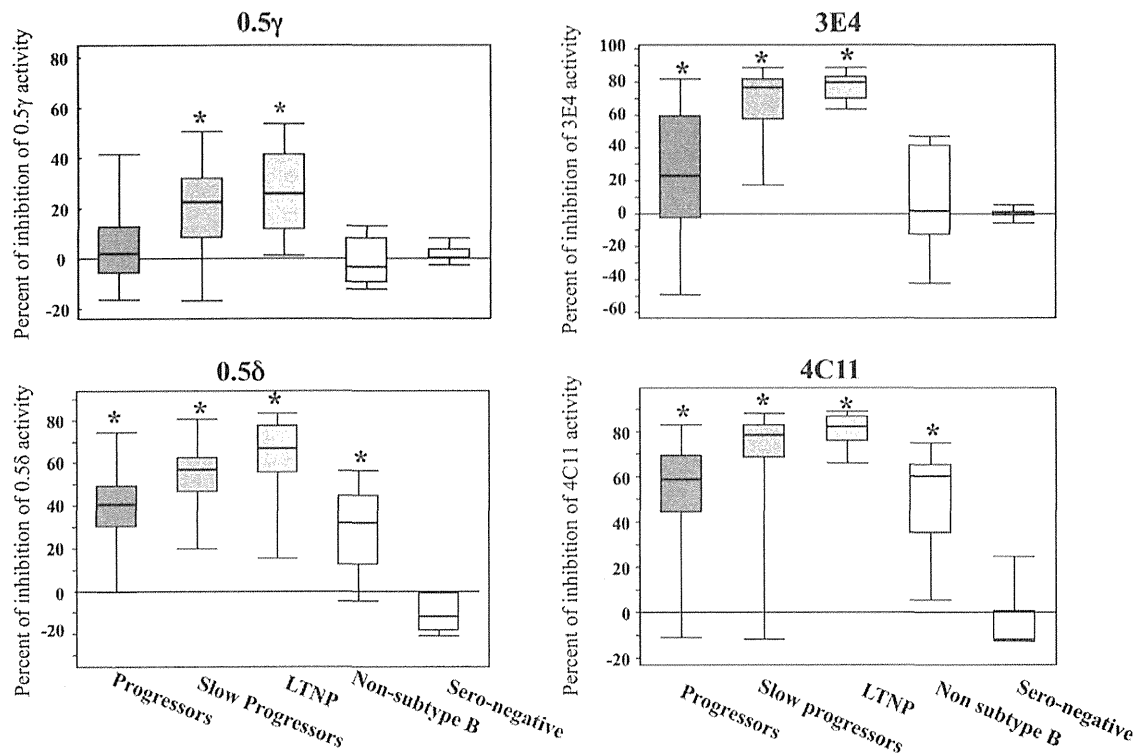
Fig. 9. Induction of antibodies with the specificity similar to MAbs from KTS376 in HIV-1-infected patients. Competition ELISA was performed using biotin-conjugated MAbs, 0.5γ, 3E8, 0.5δ and 4C11, and plasma samples (1:50 dilution) as a competitor. Plasma samples were obtained from progressors (N=47), slow progressors (N=25), Long-term non-progressors (LTNP, N=20), Non-subtype B infection (N=11) and sero-negative (N=7) individuals. Asterisks correspond to values statistically different from those of sero-negative individuals (p < 0.05) calculated by Student's t-test. The estimated time of infection with HIV-1 of patients from the long-term non-progressor group and the slow progressor group were 23 and 15 year, respectively. Time of infection for the other groups is not available.

KTS376 suggests that the humoral response played an important role in the long-term suppression of the patient. However, we cannot rule out other mechanisms, such as cellular response and viral fitness. The moderate neutralizing potency and breadth indicates that these MAbs are not classified as broad neutralizing antibodies, but rather as "conventional antibodies". This type of antibodies was recently described by Zolla-Pazner, as antibodies that have limited breadth and potency in standard neutralization assays and are commonly induced in HIV-1-infected patients. Conventional antibodies are frequently elicited during infection, and induced by many vaccine candidates tested to date, but none have yet induced broadly reactive neutralizing antibodies (Zolla-Pazner, 2014). Although each conventional antibody has only a limited breadth in neutralization, the considerable cross-reactivity of MAbs from patient KTS376, indicates that conventional antibodies can cover a wide range of viruses.

Anti-V3 MAbs had the higher frequency and potency of neutralizing activity when compared with MAbs from other specificity, especially against subtype B viruses. V3 is highly immunogenic and it is estimated that about half of the antibody responses against HIV-1 Env in patient serum is directed against this region (Javaherian et al., 1989; Moore et al., 1994; Zolla-Pazner, 2004) and at a sequence level, V3 is more conserved in comparison with the other variable regions of gp120 (Jiang et al., 2010). The anti-V3 MAbs 0.5γ and 1D9 showed the broadest neutralizing activities, comparable to that of other anti-V3 MAbs with cross-reactivity, as previously reported (Andrabi et al., 2013). MAb 16G6 has a remarkable cross-binding activity, consistent with reports of anti-V3 antibodies derived from the VH5-51 gene (Gorny et al., 2011). However, 16G6 has a weak neutralizing activity and this may be related with its low somatic mutation percentage. Despite the fact that anti-V3 MAbs frequently depend on the "GPGR" motif in the V3 tip, viruses with a different motif,

such as CH040 (GPGQ) and CH077 (GALR), were neutralized by these V3 MAbs. The induction of such antibodies with a relatively broad reactivity may require new approaches for designing V3-scaffold immunogens and adjuvants based on previous observations (Zolla-Pazner et al., 2011). In addition, the high frequency of 0.5γ-like antibodies in LTNP suggests that maturation of B cells, which is much shorter than those for bNAbs, may be important to induce V3 antibodies with cross-reactivity.

CD4bs MAbs are reported as the earliest cross-neutralizing response in patients (Andrabi et al., 2013; Jiang et al., 2010; Zolla-Pazner et al., 2011) and is not rare to found them in HIV patients' sera. Patient KTS376 was not the exception and several CD4bs MAbs with cross-neutralizing activity, even against non-B subtype viruses, were isolated. However, as it is also observed for antibodies other than CD4bs, higher concentration of antibody was required for efficient neutralization. These types of antibodies could also contribute to enhancing the V3 MAbs response, as was observed when the anti-V3 0.5γ was combined with the CD4bs MAb 0.5δ, showing the complementary and synergistc potential of CD4bs MAb. Synergy of antibodies was reported to contribute to HIV-1 control in a vaccine study (Pollara et al., 2014), and in this study we showed that synergy was also observed in a combination of antibodies derived from a single donor. This suggests that this synergy phenomenon can contribute to suppression of HIV-1 in vivo.

CD4i MAbs are induced quite frequently in HIV-1-infected patients (Decker et al., 2005). CD4i MAbs isolated from patient KTS376 were not as potent as the V3 MAbs, but were able to neutralized viruses that were not covered by anti-V3 and CD4bs MAbs; thus providing a complementarity to the antibody set. Identification of at least four lineages of CD4i antibodies, which were revealed from a genetic analysis of light chain genes, indicates the vigorous induction of CD4i antibodies in this patient.

CD4i antibodies may not contribute significantly to protection from HIV-1 infection, but may play an important role in controlling HIV-1 replication after HIV-1 infection. Some CD4i antibodies bound to a hybrid epitope conformed by the CD4 and the gp120, and for these antibodies, the presence of CD4 is indispensable for binding (Lewis et al., 2011). However, our MAbs were able to bind to gp120 even without CD4, which suggests that some part of the epitope may be exposed even before binding to CD4.

Low somatic hypermutation rates of MAbs from patient KTS376 contrasts with those of the bNAbs. A high mutation percentage is a consequence of the affinity maturation of antibodies, and is one of the main obstacles for induction of bNAbs by vaccination. In fact, a positive correlation between the level of somatic hypermutation and the development of strength and breadth of the neutralizing activity of an antibody was reported (Sok et al., 2013). However, our data show that MAbs even with low levels of affinity maturation are capable of binding and neutralizing a wide range of viruses, when antibodies targeting V3, CD4bs and CD4i acted complementarily and we observed also synergy. Synergy of neutralizing activity by two antibodies with different specificity has been already reported. Pollara et al. (2014) recently showed that C1 and V2 monoclonal antibodies isolated from RV144 vaccinees have synergistic activities for neutralization, infectious virus capture, and ADCC, and proposed that synergy among antibodies with different epitope specificities contributes to HIV-1 antiviral antibody responses. Although it is difficult to compare our results with the results reported by them due to the use of different experimental settings, they showed a 20- to 65-fold decrease of $IC_{50}s$ by combination of antibodies.

Besides neutralizing activity of the antibodies, ADCC activity has been reported to have great importance in the protection and control of the HIV-1 infection (Haynes et al., 2012a; Rerks-Ngarm et al., 2009; Wren et al., 2012). Antibodies with ADCC activity tend to have cross- or broad- activity (Smalls-Mantey et al., 2012). In addition, ADCC-mediated natural killer cell activation was significantly broader and stronger in HIV controllers than in HIV progressors (Madhavi et al., 2014). We showed significant ADCC activities of MAbs against various viruses, especially T/F viruses. The in vitro evaluation of ADCC presents certain obstacles, and one of them is a lack of suitable target cells. We used CEM.NKr.CCR5 cells as target cells, but the susceptibility of these cells to HIV-1 infection is not high due to the presence of restriction factors (Han et al., 2008). This limited the number of primary isolates evaluated, because infections could not be established for many viruses. The factors behind the presence or magnitude of the ADCC responses are not fully understood. It was reported that neutralizing and gp120 titers did not predict ADCC activity (Alpert et al., 2012). Although binding to Env is necessary for ADCC activity, we cannot observe a correlation between these two factors. Interaction of gp120 with CD4 was shown to changed ADCC activity (Veillette et al., 2014) and this could have important implications for the conformational status of Env in the infected cells. Possible causes may include the interactions between epitope and paratope and the differences in the level of epitope expression required for ADCC activity. However, the exact reasons behind this lack of correlation among binding, neutralizing and ADCC activities remains unclear, and will be a topic of future research.

A wide coverage of HIV-1 viruses by bNAbs has been previously reported (Walker et al., 2011) and great effort is invested in developing this type of antibodies by vaccination (Zolla-Pazner, 2014); however, this study supports the rationale that "conventional antibodies" are capable to provide considerable levels of coverage, as we observed that the antibodies derived from a single patient had complementary and synergistic neutralizing activity and ADCC activity. The use of mixture of Env had been proposed as

a way to achieve the induction of polyclonal response in animal models (Nkolola et al., 2014; Seaman et al., 2007, 2005). Although the induction of antibodies to specific epitopes will require further studies, antibody induction to a specific epitope was demonstrated using the antigen containing epitope with scaffold (Zolla-Pazner et al., 2011). Elicitation of antibodies with characteristics similar to MAbs from this patient, which is much easier than elicitation of highly mutated bNAbs, could be a strategy for developing an effective vaccine against HIV-1.

Material and methods

Study participant

B cells were isolated from patient KTS376. During the period of B cell isolation, CD4 cells count was above 200/µl (mean of 17 visits; 297/µl) and viral load was below 200 copies/ml (mean of 17 visits; 44.3 copies/ml), and the time frame corresponded to 23 to 28 years after infection with HIV-1. Also, KTS376 did not receive any antiretroviral treatment and besides having Hepatitis C virus co-infection, did not present any symptoms or signs of immunodeficiency. Human blood samples were collected from KTS376 after signed informed consent in accordance with the study protocol and informed consent was reviewed and approved by the Ethics committee for clinical research & advanced medical technology at the Kumamoto University Medical School.

Cells, reagents and viruses

TZM-bl (Derdeyn et al., 2000; Lambotte et al., 2009; Platt et al., 1998; Takeuchi et al., 2008; Wei et al., 2002), 293A (Life Technologies, Carlsbad, CA) and 293T (Graham et al., 1977) cells were maintained in Dubelcco's modified Eagle medium (DMEM; Sigma, St. Louis, MO) and supplemented with 10% heat-inactivated fetal calf serum (FCS; Thermo Scientific, Waltham, MA). CEM.NKr.CCR5 cells (Howell et al., 1985; Lyerly et al., 1987; Trkola et al., 1999) were maintained in RPMI-1640 medium (Sigma, St. Luis MO) supplemented with 10% FCS. PM1/CCR5 cells (Monde et al., 2007) were maintained in RPMI-1640 supplemented with 10% FCS and 100 µg/ml of G418 sulfate (Calbiochem-EMD Millipore, Billerica, MA). PM1/CCR5 cells chronically infected with HIV-1$_{JR-FL}$ were maintained in RPMI-1640 supplemented with 10% FCS. Recombinant human soluble CD4 (sCD4) was purchased from R&D systems (Minneapolis, MN). The primary HIV-1 strains, MOKW, YKI, KKGO, KMT and KTS376-96 were isolated from drug-naïve Japanese patients (Maeda et al., 2001). These viruses were passaged in phytohemagglutinin (PHA)-activated peripheral blood mononuclear cells (PBMCs) and the culture supernatant was stored at −80 °C until use. KD-247, an anti-V3 humanized mouse antibody, was produced by transferring the complementary region genes from the mouse hybridoma clone C25 into genes of the human V region as previously described (Eda et al., 2006b). CD4i MAb 17b was a kind gift from J. Robinson (Department of Pediatrics, Tulane University Medical Center, New Orleans, LA). CD4bs VRC01 was produced by Freestyle 293 expression system (Invitrogen, Life Technologies, Carlsbad, CA). Env plasmids of the Standard Virus Panel for subtype B and C strains (Li et al., 2006, 2005) were used for pseudovirus preparation and flow cytometry analysis. TZM-bl cells, CEM.NKr.CCR5 cells, VRC01 plasmid, SPVB and SPVC Env plasmids, and T/F plasmids were obtained through the NIH AIDS Reagent program, Division of AIDS, NIAID, NIH, by the kind contribution from Dr. John C. Kappes, Dr. Xiaoyun Wu, Tranzyme Inc., Dr. D. Montefiori, Dr. F. Gao, and Dr. Christina Ochsenbauer.

Pseudovirus and infectious molecular clones preparation

Pseudoviruses were prepared by transfecting exponentially dividing 293T cells with 5 μg of rev/env expression plasmid and 10 μg of an env-deficient HIV-1 backbone vector (pSG3ΔEnv), using Lipofectamin 2000 transfection reagent (Invitrogen, Life Technologies, Carlsbad, CA). Pseudovirus-containing culture supernatants were harvested 48 h after transfection, filtered (0.45 μm), and stored at −80 °C until use. Plasmids from the transmitted/founder viruses pWITO.c/2474, pCH058.c/2960, pRHPA.c/2635, pREJO.c/2864, pTRJO.c/2851, pCH106.c/2633, pCH040.c/2625, pCH077.t/2627, pSUMA.c/2821, and pTHRO.c/2626 (Keele et al., 2008; Lee et al., 2009; Salazar-Gonzalez et al., 2009, 2008) were used for producing infectious molecular clones by transfecting 5 μg of plasmid to 293T cells as described above.

Monoclonal antibody isolation

Transformation of B-cells with Epstein-Barr virus (EBV) and subsequent cloning were performed as previously described elsewhere (Matsushita et al., 1986). PBMC were separated from a patient with hemophilia A (KTS376) who had been infected with HIV-1 for more than 25 years without any antiretroviral treatment, by density gradient centrifugation of heparinized blood using Ficoll-paque (GE Healthcare, Cleveland, OH). Supernatants from individual clones was screened for the presence of IgG antibody that binds to the monomeric SF2 gp120 in a gp120 capture assay (Moore et al., 1994). Briefly, gp120 from SF2 (Austral Biologicals, San Ramon, CA) was captured onto solid phase via their carboxyl termini using sheep polyclonal antibody D7324 (Aalto Bioreagents, Dublin, Ireland). Supernatant samples were added to wells and IgG bound to gp120 was detected with alkaline phosphatase-conjugated goat anti-human IgG (Sigma, St. Luis MO) followed by addition of phosphatase substrate (Sigma, St. Luis MO). A_{405} measurements were taken using a microplate reader (Biorad, Hercules, CA).

Construction of recombinant IgG

Recombinant IgG from antibodies 16G6, 1D9 and 7171G2 were constructed as described some lines below, and used exclusively in the posterior analysis. RNA was extracted from B cells of interest with the RNeasy mini kit (Qiagen, Venlo, Netherlands). First-strand cDNA was synthesized using oligo(dT)20 (Toyobo, Osaka, Japan) and the SuperScript III Reverse transcriptase (Invitrogen, Life Technologies, Carlsbad, CA). The heavy chain variable regions were amplified using the following primers, LH1 (5′-TGG TGG CAG CAG CCA CCG GTG CCC ACT CCC AGG TGC AG-3′), LH3 (5′-TGG TGG CAG CAG CCA CCG GTG TCC AGT GTG ARG TGC AG-3′), LH46 (5′-TGG TGG CAG CAG CCA CCC GGG TCC TGT CCC AGG TGC AG-3′), LH5 (5′-TGG TGG CAG CAG CCA CCG GAG TCT GTT CCG AGG TGC AG-3′) and APS-R (5′-GGG GGA AGA CCG ATG GGC-3′). The light chain κ variable regions were amplified using primers, GKV1 (5′-GGT GCC TAC GGG GAT ATC CAG ATG ACC CAG TCT CC-3′), GKV24 (5′-GGT GCC TAC GGG GAT ATT GTG ATG ACY CAG TCT CC-3′), GKV3 (5′-GGT GCC TAC GGG GAT ATT GTG WTG ACR CAG TCT CC-3′), GKV5 (5′-GGT GCC TAC GGG GAT ACG ACA CTC ACG CAG TCT CC-3′) and HCK5-B (5′-GAA GAC AGA TGG TGC AGC CAC AGT-3′). The light chain λ variable regions were amplified using primers, LLS1 (5′-ACT TTC TGC ACA GGC TCC TGG GCC CAG TCT GTG CTG-3′), LLS2 (5′-ACT TTC TGC ACA GGC TCC TGG GCC CAG TCT GCC CTG-3′), LLS3 (5′-ACT TTC TGC ACA GGC TCT GTG ACC TCC TAT GAG CTG-3′), LLS45 (5′-ACT TTC TGC ACA GGC TCT CTC TCS CAG CYT GTG CTG-3′), LLS6 (5′-ACT TTC TGC ACA GGC TCT TGG GCC AAT TTT ATG CTG-3′), LLS7 (5′-ACT TTC TGC ACA GGC TCC AAT TCY CAG GCT GTG GTG-3′), and LLS8 (5′-ACT TTC TGC ACA GGC GTG GAT TCT CAG

ACT GTG GTG-3′) and VL-R (5′-CAG TGT GGC CTT GTT GGC TTG-3′). Polymerase chain reaction (PCR) was performed using the following conditions by Platinum Taq DNA Polymerase High Fidelity (Invitrogen, Life Technologies, Carlsbad, CA)): 94 °C for 30 s, followed by 35 cycles of 94 °C for 15 s, 55 °C for 15 s, and 68 °C for 60 s. The PCR products of the heavy chain, light chain κ and light chain λ were cloned into vectors pIgGH, pKVA2 and pLSH, respectively, using the GeneArt Seamless Cloning and Assembly kit (Invitrogen, Life Technologies, Carlsbad, CA). The vector pIgGH was basically constructed from pIgG (Rader et al., 2002), pHCG (Kuwata et al., 2011) and the plasmid to produce MAb 1C10 (0.5γ) heavy chain fragment. Briefly, the VH gene was amplified from a B cell line producing MAb 1C10 with primers HFabVH3a-F and HFabVHJa-B (Barbas et al., 2001). The CH1 region was amplified using pCOMB3XTT and primers, HIgGCH1-F and dpseq (Barbas et al., 2001). These PCR products were combined by PCR with primers SgrVH135F (5′-GCC ACC GGT GCC CAC TCC SAG GTG CAG CTG KTG-3′) and dpsp-R (5′-CAG TTT AAA CCT AAG AAG CGT AGT CCG GAA C-3′). The connected PCR product was digested with *SgrAI* and *ApaI* and inserted into pHCG. The resulting p1C10Fab to produced the 1C10 heavy chain fragment. The *XbaI-ApaI* fragment from pCOMB3XSS and the *ApaI-PmeI* fragment from the PCR product, which was amplified using primers, HIgGH1-F (5′-GCC TCC ACC AAG GGC CCA TCG GTC-3′) and CH-R (5′-AGG TTT ACT AGT ACC ACC ACA TGT TTT TAT CTC-3′), and pIgG as a template, were inserted into p1C10Fab. The resultant pIgGH has the signal peptide region and the constant regions of IgG, and was used to clone VH genes after removing the stuffer sequence by digestion with *SgrAI* and *ApaI*. The vector pKVA2 was constructed by insertion of two PCR products into pcDNA3.1/Hygro(+) (Invitrogen, Life Technologies, Carlsbad, CA) and was used to clone VK genes after digestion with *EcoRV* and *AfeI*. The signal peptide region was amplified using the primers, SPKNH-F (5′-AAG CTA GCA TGG TGT TGC AGA C-3′) and SPKEV-R (5′-AAG ATA TCC CCG TAG GCA CCA GAG-3′), and pIgG as a template, and the *NheI-EcoRV* fragment was used for the insertion. The light chain κ constant region was amplified using the primers, EcVAfe-F (5′-CCG ATA TCT TAG CGC TGC ACC ATC TGT CTT C-3′) and BGH-R (5′-TAG AAG GCA CAG TCG AGG-3′), and p1C10L, which had the *HindIII-XbaI* fragment containing MAb 1C10 light chain in pcDNA3.1/Hygro(+). The vector pLSH was constructed by inserting the *HindIII-HpaI* fragment and the *HpaI-XbaI* fragment, which were amplified using p916B2L and primer pairs, T7-F and HpaSfo-R, and Hpa-F and BGH-R, respectively, into pcDNA3.1/Hygro(+). The plasmid p916B2L was constructed by inserting the *NheI-XbaI* fragment, which contained the signal peptide region from pLL-B404 to producing the light chain of MAb B404 (Kuwata et al., 2011) and the light chain λ gene from MAb 916B2, into pcDNA3.1/Hygro(+). Plasmids, pIgG, pCOMB3XSS and pCOMB3XTT were kindly provided from Dr. Barbas (The Scripps Research Institute).

Recombinant antibodies were obtained by co-transfection of heavy and light chain plasmids to 293A cells (Life Technologies, Carlsbad, CA) and cells stably expressing antibodies were selected with G418 (800 μg/ml) and Hygromycin (160 μg/ml). The nucleotide sequence of MAbs was determined using a Big Dye Terminator, version 1.1 (Applied Biosystems, Life Technologies, Carlsbad, CA) and the genetic analyzer A&B 3500/3500xL (Applied Biosystems, Life Technologies, Carlsbad, CA). Sequences were aligned and analyzed using the CLC Sequence viewer 6 (CLCbio, Boston, MA). Evolutionary analyses were conducted in MEGA5 (Tamura et al., 2011).

Binding activity of MAbs to HIV-1 Env by ELISA analysis

Capture ELISA described in the previous section and Flow cytometry were used to determine the binding of the MAbs to

monomeric and trimeric gp120, respectively. The effect of sCD4 (2 µg/ml) over binding to gp120 and binding to V3 peptide allowed classifying the MAbs into four groups: V3, CD4bs, CD4i and "other epitopes" MAbs.

Reactivity of V3 MAbs against a panel of known V3 epitopes was performed using a peptide-based ELISA as described elsewhere (Eda et al., 2006b). Briefly, synthetic V3 peptides in PBS (1 µg/ml) were pre-coated in polyvinyl chloride flexible 96 well plates (BD Falcon, Franklin Lakes, NJ) and incubated overnight at 4 °C; later plates were blocked with 2% bovine serum albumin-0.1% Tween 20 in PBS. V3 MAbs (1 µg/ml) were added and incubated for 1 h at room temperature. IgG bound to V3 peptides was detected with alkaline phosphatase-conjugated goat anti-human IgG (Sigma, St. Luis MO) followed by addition of phosphatase substrate (Sigma, St. Luis MO). A_{405} measurements were taken using a microplate reader (Biorad, Hercules, CA).

Binding activity of MAbs to HIV-1 Env by flow cytometry analysis

The ability of MAbs to bind virus-infected cells was analyzed by flow cytometric analysis. Briefly, PM1/CCR5 cells were chronically infected with HIV-1 $_{JR-FL}$ as previously described (Yoshimura et al., 2006). Infected and uninfected cells were washed with PBS and adjusted to 5×10^6 cells/ml. For cell surface staining, 100 µl cells in PBS containing 0.2% BSA were incubated with 50 µl of 5 µg/ml MAbs for 60 min at room temperature (RT). After washing with PBS containing 0.2% BSA, cells were incubated with 50 µl of allophycocyanin (APC)-conjugated AffiniPure F(ab′)2 Fragment Goat Anti-Human IgG (H+L) (Jackson ImmunoResearch, West Grove, PA) for 30 min at RT. Cells were fixed with PBS containing 10% formalin, and analyzed by FACSCalibur instrument (Becton Dickinson, Franklin Lakes, NJ). Data analysis was performed using FlowJo (TreeStar, San Carlos, CA).

Binding to Env from various HIV-1 strains was determined using the 293T cells transfected with plasmids that expressed both Env and enhanced green fluorescent protein (EGFP). The transfected cells were incubated with antibody (5 µg/ml) for 1 h at RT. The antibody binding was detected using APC-conjugated AffiniPure F(ab′)2 Fragment Goat Anti-Human IgG (H+L) and FACSCalibur as described above.

Determination of neutralization activity

Neutralization activity was measured with a modified version of an assay described previously (Montefiori, 2009). Briefly, serial dilutions of MAbs and virus (400 Tissue Culture Infectious Dose [TCID]$_{50}$) were pre-incubated for 1 h. TZM-bl cells solution containing DEAE-dextran (25 µg/ml) were added and incubated for 48 h (37 °C and 5% CO_2), washed with PBS and lysed with lysis buffer (Galacto-star system, Life technologies, Carlsbad, CA). Lysate was transferred to an opaque plate containing β-galactosidase substrate (Galacto-star system, Life technologies, Carlsbad, CA) and incubated for 1 h. The β-galactosidase activity was measured in relative light units (RLU) using a Centro XS^3 LB960 luminometer (Berthold technologies, Bad Wildbad, Germany). The reduction of infectivity was determined by comparing the RLU in the presence and absence of antibody and was expressed as a percentage of neutralization.

Antibody-dependent cell-mediated cytotoxicity (ADCC) assay

ADCC activity was addressed using the rapid fluorometric assessment of ADCC (RFADCC) previously reported elsewhere (Gómez-Román et al., 2006). Target cells were CEM.NKr.CCR5 cells which were chronically infected with different strains of HIV-1. The gp120 coated cells were prepared by incubating 5×10^6 cells

with 15 µg of gp120 for 1 h. Cells were washed twice in ice-cold medium and coating was confirmed by binding of VRC01 to Env using flow cytometry. The infected cells were prepared by infection 7 days prior to the assay by spinoculation (O'Doherty et al., 2000). Briefly, a mixture of 5×10^5 cells, viral inoculum and polybrene were centrifuged for 2 h at $1200 \times g$ at 25 °C. Then, cells were cultured in RPMI supplemented with 10% FCS and media was exchanged every 48 h. Envelope expression was confirmed by binding of VRC01 using flow cytometry. PBMC or NK enriched-PBMC were used as effector cells. The NK enriched-PBMC fraction was prepared by using the NK cell isolation kit (Miltenyi Biotec, Bergisch Gladbach, Germany). Target cells were stained with carboxyfluorescein succinimidyl ester (CFSE; (Invitrogen, Life Technologies, Carlsbad, CA) and PKH-26 (Sigma, St. Luis, MO) according to the manufacturer's instructions. Stained cells were re-suspended and 50 µl (5000 cells) were incubated with 100 µl of antibody for 1 h at room temperature. Different concentrations were tested for each antibody in order to determine the optimal concentration for each antibody-virus combination. Then, 50 µl of effector cells were added to reach an Effector:Target ratio of 50:1 for PBMC and 5:1 for NK-enriched PBMC. Plates were centrifuged for 3 min at $400 \times g$ and incubated for 6 h (37 °C and 5% CO_2). Finally, cells were washed with PBS, and fixed with PBS containing 10% formalin. Data was acquired with a FACSCalibur instrument and analyzed with FlowJo software. ADCC activity was calculated as follows: first PKH-26 positive cells were gated (target cells), later the percentage of death dead cells (i.e. that have lost the CFSE dye, CFSE-) was determined. In each experiment, the percentage of killing obtained from target and effector cells without antibody was denoted as "background killing" and was subtracted from all the samples. Representative dot plots can be found in the supplementary data section (Supplementary Figs. 3 and 4) Differences in the ADCC activity of the negative control (8D11) and the samples were evaluated using the Mann–Whitney U test (Wilcoxon rank-sum test) with a 95% confidence interval. Differences were considered significant if p was < 0.05. The test was performed using the GraphPad Prism 6 software (GraphPad Software, La Jolla, CA).

Evaluation of MAbs synergistic effect

We first tested the binding activity of MAbs in the presence or absence of 0.5δ using a gp120 capture ELISA as described above. Briefly, plates covered with gp120 SF2 were incubated for 30 min with 50 µl of 0.5δ. Later, 50 µl of biotin-conjugated MAbs at a concentration of 1 µg/m were dispensed in each well. We also tested the combination effect of MAbs over neutralization by using the neutralization assay described above. Briefly, serial dilutions of MAbs and 0.5δ in 1:1 combination ratio and virus (400 TCID$_{50}$) were pre-incubated for 1 h. TZM-bl cells solution containing DEAE-dextran (25 µg/ml) were added and incubated for 48 h (37 °C and 5% CO_2), washed with PBS and lysed with lysis buffer (Galacto-star system, Life technologies, Carlsbad, CA). Lysate was transferred to an opaque plate containing β-galactosidase substrate (Galacto-star system, Life technologies, Carlsbad, CA) and incubated for 1 h. The β-galactosidase activity was measured in relative light units (RLU) using a Centro XS^3 LB960 luminometer (Berthold technologies, Bad Wildbad, Germany). The reduction of infectivity was determined by comparing the RLU in the presence and absence of antibody and was expressed as a percentage of neutralization. Combination and synergistic effect of 0.5γ with 0.5δ was analyzed by the Chou and Talaly (1977) method and 3 dimensional analyses. Using the CalcuSyn version 2 software, combination indices (CI) were calculated using the MAbs Inhibitory Concentrations (IC) and interpreted as follows: CI < 0.9

synergy, $0.9 < CI < 1.1$ additivity and $CI > 1.1$ antagonism (Maeda et al., 2001; Yoshimura et al., 2006).

Competitive binding assay

Selected MAbs 0.5γ (V3), 3E4 (V3), 0.5δ (CD4bs) and 4C11 (CD4i) were conjugated with biotin and subjected for evaluation of epitope-competing antibodies in plasma samples from HIV-1 infected patients, using a gp120 capture ELISA as described above. Briefly, plates covered with gp120 SF2 were incubated for 30 min with 50 μl of 3 fold serial dilution of plasma samples. Later, 50 μl of biotin-conjugated MAbs at a concentration of 1 μg/m were dispensed in each well. The competition in binding of each biotin-conjugated MAb was detected by ALP- conjugated Avidin (Sigma, St. Luis MO) and substrate.

We evaluated the existence of epitope-competing antibodies in patients' plasma samples including 47 from ordinary progressors, 25 from slow-progressors, 20 from non-progressors, 11 from non-subtype B virus infection and 7 from seronegative donors in this competition assay using 1:50 dilution of the plasma. Plasma samples of non-progressors were collected from hemophiliac patients in Japan who kept CD4$^+$ cells counts higher than 350/μl without antiviral treatment at 2005, the time frame estimated for 23 years of HIV-infection. Plasma samples of slow progressors were collected from hemophiliac patients in Japan who started antiviral treatment with CD4$^+$ cell counts at 350–200/μl after 1997, the time estimated for more than 15 years of HIV-infection. Ordinary progressors are patients with subtype B infection who had initiated antiviral treatment with CD4$^+$ cells counts less than 200/μl.

Acknowledgments

Appendix A. Supporting information

Supplementary data associated with this article can be found in the online version at http://dx.doi.org/10.1016/j.virol.2014.11.011.

References

Alpert, M.D., Heyer, L.N., Williams, D.E.J., Harvey, J.D., Greenough, T., Allhorn, M., Evans, D.T., 2012. A novel assay for antibody-dependent cell-mediated cytotoxicity against HIV-1- or SIV-infected cells reveals incomplete overlap with antibodies measured by neutralization and binding assays. J. Virol. 86, 12039–12052. http://dx.doi.org/10.1128/JVI.01650-12.

Andrabi, R., Williams, C., Wang, X.-H., Li, L., Choudhary, A.K., Wig, N., Biswas, A., Luthra, K., Nadas, A., Seaman, M.S., Nyambi, P., Zolla-Pazner, S., Gorny, M.K., 2013. Cross-neutralizing activity of human anti-V3 monoclonal antibodies derived from non-B clade HIV-1 infected individuals. Virology 439, 81–88. http://dx.doi.org/10.1016/j.virol.2012.12.010.

Banerjee, K., Klasse, P.J., Sanders, R.W., Pereyra, F., Michael, E., Lu, M., Walker, B.D., Moore, J.P., 2010. IgG subclass profiles in infected HIV type 1 controllers and chronic progressors and in uninfected recipients of Env vaccines. AIDS Res. Hum. Retroviruses 26, 445–458. http://dx.doi.org/10.1089/aid.2009.0223.

Bar, K.J., Tsao, C., Iyer, S.S., Decker, J.M., Yang, Y., Bonsignori, M., Chen, X., Hwang, K.-K., Montefiori, D.C., Liao, H.-X., Hraber, P., Fischer, W., Li, H., Wang, S., Sterrett, S., Keele, B.F., Ganusov, V.V., Perelson, A.S., Korber, B.T., Georgiev, I., McLellan, J.S., Pavlicek, J.W., Gao, F., Haynes, B.F., Hahn, B.H., Kwong, P.D., Shaw, G.M., 2012. Early low-titer neutralizing antibodies impede HIV-1 replication and select for virus escape. PLoS Pathog. 8, e1002721. http://dx.doi.org/10.1371/journal.ppat.1002721.

Barbas III, C.F., Burton, D.R., Scott, J.K., Silverman, G.J., 2001. Phage Display: A Laboratory Manual. Cold Spring Harbor Laboratory Press, Cold Spring Harbor, New York.

Barouch, D.H., Whitney, J.B., Moldt, B., Klein, F., Oliveira, T.Y., Liu, J., Stephenson, K.E., Chang, H.-W., Shekhar, K., Gupta, S., Nkolola, J.P., Seaman, M.S., Smith, K.M., Borducchi, E.N., Cabral, C., Smith, J.Y., Blackmore, S., Sanisetty, S., Perry, J.R., Beck, M., Lewis, M.G., Rinaldi, W., Chakraborty, A.K., Poignard, P., Nussenzweig, M.C., Burton, D.R., 2013. Therapeutic efficacy of potent neutralizing HIV-1-specific monoclonal antibodies in SHIV-infected rhesus monkeys. Nature 503, 224–228.

Binley, J.M., Lybarger, E.A., Crooks, E.T., Seaman, M.S., Gray, E., Davis, K.L., Decker, J.M., Wycuff, D., Harris, L., Hawkins, N., Wood, B., Nathe, C., Richman, D., Tomaras, G.D., Bibollet-Ruche, F., Robinson, J.E., Morris, L., Shaw, G.M., Montefiori, D.C., Mascola, J.R., 2008. Profiling the specificity of neutralizing antibodies in a large panel of plasmas from patients chronically infected with human immunodeficiency virus type 1 subtypes B and C. J. Virol. 82, 11651–11668. http://dx.doi.org/10.1128/JVI.01762-08.

Bonsignori, M., Hwang, K.-K., Chen, X., Tsao, C.-Y., Morris, L., Gray, E., Marshall, D.J., Crump, J.A., Kapiga, S.H., Sam, N.E., Sinangil, F., Pancera, M., Yongping, Y., Zhang, B., Zhu, J., Kwong, P.D., O'Dell, S., Mascola, J.R., Wu, L., Nabel, G.J., Phogat, S., Seaman, M.S., Whitesides, J.F., Moody, M.A., Kelsoe, G., Yang, X., Sodroski, J., Shaw, G.M., Montefiori, D.C., Kepler, T.B., Tomaras, G.D., Alam, S.M., Liao, H.-X., Haynes, B.F., 2011. Analysis of a clonal lineage of HIV-1 envelope V2/V3 conformational epitope-specific broadly neutralizing antibodies and their inferred unmutated common ancestors. J. Virol. 85, 9998–10009. http://dx.doi.org/10.1128/JVI.05045-11.

Boyer, S., 2009. Financial barriers to HIV treatment in Yaounde, Cameroon: first results of a national cross-sectional survey. Bull. World Health Organ., 87; , pp. 279–287. http://dx.doi.org/10.2471/BLT.07.049643.

Burton, D.R., Barbas, C.F., Persson, M.a., Koenig, S., Chanock, R.M., Lerner, R.a., 1991. A large array of human monoclonal antibodies to type 1 human immunodeficiency virus from combinatorial libraries of asymptomatic seropositive individuals. Proc. Natl. Acad. Sci. U.S.A. 88, 10134–10137.

Buzon, M.J., Massanella, M., Llibre, J.M., Esteve, A., Dahl, V., Puertas, M.C., Gatell, J.M., Domingo, P., Paredes, R., Sharkey, M., Palmer, S., Stevenson, M., Clotet, B., Blanco, J., Martinez-Picado, J., 2010. HIV-1 replication and immune dynamics are affected by raltegravir intensification of HAART-suppressed subjects. Nat. Med. 16, 460–465.

Choe, H., Li, W., Wright, P.L., Vasilieva, N., Venturi, M., Huang, C.-C., Grundner, C., Dorfman, T., Zwick, M.B., Wang, L., Rosenberg, E.S., Kwong, P.D., Burton, D.R., Robinson, J.E., Sodroski, J.G., Farzan, M., 2003. Tyrosine sulfation of human antibodies contributes to recognition of the CCR5 binding region of HIV-1 gp120. Cell 114, 161–170.

Chou, T.C., Talaly, P., 1977. A simple generalized equation for the analysis of multiple inhibitions of Michaelis–Menten kinetic systems. J. Biol. Chem. 252, 6438–6442.

Corti, D., Langedijk, J.P.M., Hinz, A., Seaman, M.S., Vanzetta, F., Fernandez-Rodriguez, B.M., Silacci, C., Pinna, D., Jarrossay, D., Balla-Jhagjhoorsingh, S., Willems, B., Zekveld, M.J., Dreja, H., O'Sullivan, E., Pade, C., Orkin, C., Jeffs, S.a., Montefiori, D.C., Davis, D., Weissenhorn, W., McKnight, A., Heeney, J.L., Sallusto, F., Sattentau, Q.J., Weiss, R.a., Lanzavecchia, A., 2010. Analysis of memory B cell responses and isolation of novel monoclonal antibodies with neutralizing breadth from HIV-1-infected individuals. PLoS One 5, e8805. http://dx.doi.org/10.1371/journal.pone.0008805.

Decker, J.M., Bibollet-Ruche, F., Wei, X., Wang, S., Levy, D.N., Wang, W., Delaporte, E., Peeters, M., Derdeyn, C.A., Allen, S., Hunter, E., Saag, M.S., Hoxie, J.A., Hahn, B.H., Kwong, P.D., Robinson, J.E., Shaw, G.M., 2005. Antigenic conservation and immunogenicity of the HIV coreceptor binding site. J. Exp. Med. 201, 1407–1419 http://dx.doi.org/10.1084/jem.20042510.

Deeks, S.G., Schweighardt, B., Wrin, T., Galovich, J., Hoh, R., Sinclair, E., Hunt, P., McCune, J.M., Martin, J.N., Petropoulos, C.J., Hecht, F.M., 2006. Neutralizing antibody responses against autologous and heterologous viruses in acute versus chronic human immunodeficiency virus (HIV) infection: evidence for a constraint on the ability of HIV to completely evade neutralizing antibody responses. J. Virol. 80, 6155–6164. http://dx.doi.org/10.1128/JVI.00093-06.

Derdeyn, C.A., Decker, J.M., Sfakianos, J.N., Wu, X., Brien, W.A.O., Ratner, L., John, C., Shaw, G.M., Hunter, E., O'Brien, W.A., Kappes, J.C., 2000. Sensitivity of human immunodeficiency virus type 1 to the fusion inhibitor T-20 is modulated by coreceptor specificity defined by the V3 loop of gp120. J. Virol. 74, 8358–8367. http://dx.doi.org/10.1128/JVI.74.18.8358-8367.2000.

DeVico, A., Fouts, T., Lewis, G.K., Gallo, R.C., Godfrey, K., Charurat, M., Harris, I., Galmin, L., Pal, R., 2007. Antibodies to CD4-induced sites in HIV gp120 correlate with the control of SHIV challenge in macaques vaccinated with subunit

immunogens. Proc. Natl. Acad. Sci. U.S.A 104, 17477–17482. http://dx.doi.org/10.1073/pnas.0707399104.

Dhillon, A.K., Donners, H., Pantophlet, R., Johnson, W.E., Decker, J.M., Shaw, G.M., Lee, F.-H., Richman, D.D., Doms, R.W., Vanham, G., Burton, D.R., 2007. Dissecting the neutralizing antibody specificities of broadly neutralizing sera from human immunodeficiency virus type 1-infected donors. J. Virol. 81, 6548–6562. http://dx.doi.org/10.1128/JVI.02749-06.

Doria-Rose, N.A., Klein, R.M., Daniels, M.G., O'Dell, S., Nason, M., Lapedes, A., Bhattacharya, T., Migueles, S.a., Wyatt, R.T., Korber, B.T., Mascola, J.R., Connors, M., 2010. Breadth of human immunodeficiency virus-specific neutralizing activity in sera: clustering analysis and association with clinical variables. J. Virol. 84, 1631–1636. http://dx.doi.org/10.1128/JVI.01482-09.

Doria-Rose, N.A., Klein, R.M., Manion, M.M., O'Dell, S., Phogat, A., Chakrabarti, B., Hallahan, C.W., Migueles, S.a., Wrammert, J., Ahmed, R., Nason, M., Wyatt, R.T., Mascola, J.R., Connors, M., 2009. Frequency and phenotype of human immunodeficiency virus envelope-specific B cells from patients with broadly cross-neutralizing antibodies. J. Virol. 83, 188–199. http://dx.doi.org/10.1128/JVI.01583-08.

Eda, Y., Murakami, T., Ami, Y., Nakasone, T., Takizawa, M., Someya, K., Kaizu, M., Izumi, Y., Yoshino, N., Matsushita, S., Higuchi, H., Matsui, H., Shinohara, K., Takeuchi, H., Koyanagi, Y., Yamamoto, N., Honda, M., 2006a. Anti-V3 humanized antibody KD-247 effectively suppresses ex vivo generation of human immunodeficiency virus type 1 and affords sterile protection of monkeys against a heterologous simian/human immunodeficiency virus infection. J. Virol. 80, 5563–5570. http://dx.doi.org/10.1128/JVI.02095-05.

Eda, Y., Takizawa, M., Murakami, T., Maeda, H., Kimachi, K., Yonemura, H., Koyanagi, S., Shiosaki, K., Higuchi, H., Makizumi, K., Nakashima, T., Osatomi, K., Tokiyoshi, S., Matsushita, S., Yamamoto, N., Honda, M., 2006b. Sequential immunization with V3 peptides from primary human immunodeficiency virus type 1 produces cross-neutralizing antibodies against primary isolates with a matching narrow-neutralization sequence motif. J. Virol. 80, 5552–5562. http://dx.doi.org/10.1128/JVI.02094-05.

Gnanakaran, S., Daniels, M.G., Bhattacharya, T., Lapedes, A.S., Sethi, A., Li, M., Tang, H., Greene, K., Gao, H., Haynes, B.F., Cohen, M.S., Shaw, G.M., Seaman, M.S., Kumar, A., Gao, F., Montefiori, D.C., Korber, B., 2010. Genetic signatures in the envelope glycoproteins of HIV-1 that associate with broadly neutralizing antibodies. PLoS Comput. Biol. 6, e1000955. http://dx.doi.org/10.1371/journal.pcbi.1000955.

Gómez-Román, V.R., Florese, R.H., Patterson, L.J., Peng, B., Venzon, D., Aldrich, K., Robert-Guroff, M., 2006. A simplified method for the rapid fluorometric assessment of antibody-dependent cell-mediated cytotoxicity. J. Immunol. Methods 308, 53–67. http://dx.doi.org/10.1016/j.jim.2005.09.018.

Gorny, M.K., Sampson, J., Li, H., Jiang, X., Totrov, M., Wang, X.-H., Williams, C., O'Neal, T., Volsky, B., Li, L., Cardozo, T., Nyambi, P., Zolla-Pazner, S., Kong, X.-P., 2011. Human anti-V3 HIV-1 monoclonal antibodies encoded by the VH5-51/VL lambda genes define a conserved antigenic structure. PLoS One 6, e27780. http://dx.doi.org/10.1371/journal.pone.0027780.

Gorny, M.K., Wang, X.-H., Williams, C., Volsky, B., Revesz, K., Witover, B., Burda, S., Urbanski, M., Nyambi, P., Krachmarov, C., Pinter, A., Zolla-Pazner, S., Nadas, A., 2009. Preferential use of the VH5-51 gene segment by the human immune response to code for antibodies against the V3 domain of HIV-1. Mol. Immunol. 46, 917–926. http://dx.doi.org/10.1016/j.molimm.2008.09.005.

Graham, F.L., Smiley, J., Russell, W.C., Nairn, R., 1977. Characteristics of a human cell line transformed by DNA from human adenovirus type 5. J. Gen. Virol. 36, 59–74.

Gray, E.S., Madiga, M.C., Hermanus, T., Moore, P.L., Wibmer, C.K., Tumba, N.L., Werner, L., Mlisana, K., Sibeko, S., Williamson, C., Abdool Karim, S.S., Morris, L., Team, the C.S, 2011. The neutralization breadth of HIV-1 develops incrementally over four years and is associated with CD4+ T cell decline and high viral load during acute infection. J. Virol 85, 4828–4840. http://dx.doi.org/10.1128/JVI.00198-11.

Han, Y., Wang, X., Dang, Y., Zheng, Y.-H., 2008. Demonstration of a novel HIV-1 restriction phenotype from a human T cell line. PLoS One 3, e2796.

Haynes, B.F., Gilbert, P.B., McElrath, M.J., Zolla-Pazner, S., Tomaras, G.D., Alam, S.M., Evans, D.T., Montefiori, D.C., Karnasuta, C., Sutthent, R., Liao, H.-X.X., DeVico, A.L., Lewis, G.K., Williams, C., Pinter, A., Fong, Y., Janes, H., DeCamp, A., Huang, Y., Rao, M., Billings, E., Karasavvas, N., Robb, M.L., Ngauy, V., de Souza, M.S., Paris, R., Ferrari, G., Bailer, R.T., Soderberg, K.A., Andrews, C., Berman, P.W., Frahm, N., De Rosa, S.C., Alpert, M.D., Yates, N.L., Shen, X., Koup, R.A., Pitisuttithum, P., Kaewkungwal, J., Nitayaphan, S., Rerks-Ngarm, S., Michael, N.L., Kim, J.H., 2012a. Immune-correlates analysis of an HIV-1 vaccine efficacy trial. N. Engl. J. Med. 366 1275–1286 http://dx.doi.org/10.1056/NEJMoa1113425.

Haynes, B.F., Kelsoe, G., Harrison, S.C., Kepler, T.B., 2012b. B-cell-lineage immunogen design in vaccine development with HIV-1 as a case study. Nat. Biotechnol. 30, 423–433. http://dx.doi.org/10.1038/nbt.2197.

Hessell, A.J., Hangartner, L., Hunter, M., Havenith, C.E.G., Beurskens, F.J., Bakker, J.M., Lanigan, C.M.S., Landucci, G., Forthal, D.N., Parren, P.W.H.I., Marx, P.A., Burton, D.R., 2007. Fc receptor but not complement binding is important in antibody protection against HIV. Nature 449, 101–104. http://dx.doi.org/10.1038/nature06106.

Hessell, A.J., Poignard, P., Hunter, M., Hangartner, L., Tehrani, D.M., Bleeker, W.K., Parren, P.W.H.I., Marx, P.A., Burton, D.R., 2009a. Effective, low-titer antibody protection against low-dose repeated mucosal SHIV challenge in macaques. Nat. Med. 15, 951–954. http://dx.doi.org/10.1038/nm.1974.

Hessell, A.J., Rakasz, E.G., Poignard, P., Hangartner, L., Landucci, G., Forthal, D.N., Koff, W.C., Watkins, D.I., Burton, D.R., 2009b. Broadly neutralizing human anti-HIV antibody 2G12 is effective in protection against mucosal SHIV challenge even at low serum neutralizing titers. PLoS Pathog. 5, e1000433. http://dx.doi.org/10.1371/journal.ppat.1000433.

Hessell, A.J., Rakasz, E.G., Tehrani, D.M., Huber, M., Weisgrau, K.L., Landucci, G., Forthal, D.N., Koff, W.C., Poignard, P., Watkins, D.I., Burton, D.R., 2010. Broadly neutralizing monoclonal antibodies 2F5 and 4E10 directed against the human immunodeficiency virus type 1 gp41 membrane-proximal external region protect against mucosal challenge by simian-human immunodeficiency virus SHIVBa-L. J. Virol. 84, 1302–1313. http://dx.doi.org/10.1128/JVI.01272-09.

Howell, D., Andreotti, J., Cresswell, P., 1985. Natural killing target antigens as inducers of interferon; studies with an immunoselected, natural-killing-resistant human T-lymphoblastoid cell line. J. Immunol. 134, 971–976.

Huang, C., Tang, M., Zhang, M.-Y., Majeed, S., Montabana, E., Stanfield, R.L., Dimitrov, D.S., Korber, B., Sodroski, J., Wilson, I.A., Wyatt, R., Kwong, P.D., 2005. Structure of a V3-containing HIV-1 gp120 core. Science 310, 1025–1028. http://dx.doi.org/10.1126/science.1118398.

Huang, C., Venturi, M., Majeed, S., Moore, M.J., Phogat, S., Zhang, M.-Y., Dimitrov, D.S., Hendrickson, W.A., Robinson, J., Sodroski, J., Wyatt, R., Choe, H., Farzan, M., Kwong, P.D., 2004. Structural basis of tyrosine sulfation and VH-gene usage in antibodies that recognize the HIV type 1 coreceptor-binding site on gp120. Proc. Natl. Acad. Sci. U.S.A. 101, 2706–2711. http://dx.doi.org/10.1073/pnas.0308527100.

Huber, M., Le, K.M., Doores, K.J., Fulton, Z., Stanfield, R.L., Wilson, I.a., Burton, D.R., 2010. Very few substitutions in a germ line antibody are required to initiate significant domain exchange. J. Virol. 84, 10700–10707. http://dx.doi.org/10.1128/JVI.01111-10.

Javaherian, K., Langlois, A.J., McDanal, C., Ross, K.L., Eckler, L.I., Jellis, C.L., Profy, A.T., Rusche, J.R., Bolognesi, D.P., Putney, S.D., 1989. Principal neutralizing domain of the human immunodeficiency virus type 1 envelope protein. Proc. Natl. Acad. Sci. U.S.A 86, 6768–6772.

Jiang, X., Burke, V., Totrov, M., Williams, C., Cardozo, T., Gorny, M.K., Zolla-Pazner, S., Kong, X.-P., 2010. Conserved structural elements in the V3 crown of HIV-1 gp120. Nat. Struct. Mol. Biol. 17, 955–961. http://dx.doi.org/10.1038/nsmb.1861.

Keele, B.F., Giorgi, E.E., Salazar-Gonzalez, J.F., Decker, J.M., Pham, K.T., Salazar, M.G., Sun, C., Grayson, T., Wang, S., Li, H., Wei, X., Jiang, C., Kirchherr, J.L., Gao, F., Anderson, J.A., Ping, L.-H., Swanstrom, R., Tomaras, G.D., Blattner, W.A., Goepfert, P.a., Kilby, J.M., Saag, M.S., Delwart, E.L., Busch, M.P., Cohen, M.S., Montefiori, D.C., Haynes, B.F., Gaschen, B., Athreya, G.S., Lee, H.Y., Wood, N., Seoighe, C., Perelson, A.S., Bhattacharya, T., Korber, B.T., Hahn, B.H., Shaw, G.M., 2008. Identification and characterization of transmitted and early founder virus envelopes in primary HIV-1 infection. Proc. Natl. Acad. Sci. U.S.A 105, 7552–7557. http://dx.doi.org/10.1073/pnas.0802203105.

Klein, F., Diskin, R., Scheid, J.F., Gaebler, C., Mouquet, H., Georgiev, I.S., Pancera, M., Zhou, T., Incesu, R.-B., Fu, B.Z., Gnanapragasam, P.N.P., Oliveira, T.Y., Seaman, M.S., Kwong, P.D., Bjorkman, P.J., Nussenzweig, M.C., 2013. Somatic mutations of the immunoglobulin framework are generally required for broad and potent HIV-1 neutralization. Cell 153, 126–138. http://dx.doi.org/10.1016/j.cell.2013.03.018.

Klein, F., Halper-Stromberg, A., Horwitz, J.A., Gruell, H., Scheid, J.F., Bournazos, S., Mouquet, H., Spatz, L.A., Diskin, R., Abadir, A., Zang, T., Dorner, M., Billerbeck, E., Labitt, R.N., Gaebler, C., Marcovecchio, P.M., Incesu, R.-B., Eisenreich, T.R., Bieniasz, P.D., Seaman, M.S., Bjorkman, P.J., Ravetch, J.V., Ploss, A., Nussenzweig, M.C., 2012. HIV therapy by a combination of broadly neutralizing antibodies in humanized mice. Nature 492, 118–122. http://dx.doi.org/10.1038/nature11604.

Kuwata, T., Katsumata, Y., Takaki, K., Miura, T., Igarashi, T., 2011. Isolation of potent neutralizing monoclonal antibodies from an SIV-infected rhesus macaque by phage display. AIDS Res. Hum. Retroviruses 27, 487–500. http://dx.doi.org/10.1089/aid.2010.0191.

Kwong, P.D., Doyle, M.L., Casper, D.J., Cicala, C., Leavitt, S.A., Majeed, S., Steenbeke, T.D., Venturi, M., Chaiken, I., Fung, M., Katinger, H., Parren, P.W.I.H., Robinson, J., Ryk, D., Van, Wang, L., Burton, D.R., Freire, E., Wyatt, R., Sodroski, J., Hendrickson, W.A., Arthos, J., 2002. HIV-1 evades antibody-mediated neutralization through conformational masking of receptor-binding sites. Nature 420, 678–682 http://dx.doi.org/10.1038/nature01272.Published.

Kwong, P.D., Wyatt, R., Robinson, J., Sweet, R.W., Sodroski, J., Hendrickson, W.A., 1998. Structure of an HIV gp120 envelope glycoprotein in complex with the CD4 receptor and a neutralizing human antibody. Nature 393, 648–659. http://dx.doi.org/10.1038/31405.

Lambotte, O., Ferrari, G., Moog, C., Yates, N.L., Liao, H.-X., Parks, R.J., Hicks, C.B., Owzar, K., Tomaras, G.D., Montefiori, D.C., Haynes, B.F., Delfraissy, J.-F., 2009. Heterogeneous neutralizing antibody and antibody-dependent cell cytotoxicity responses in HIV-1 elite controllers. AIDS 23, 897–906. http://dx.doi.org/10.1097/QAD.0b013e328329f97d.

Lee, H.Y., Giorgi, E.E., Keele, B.F., Gaschen, B., Athreya, G.S., Salazar-Gonzalez, J.F., Pham, K.T., Goepfert, P.A., Kilby, J.M., Saag, M.S., Delwart, E.L., Busch, M.P., Hahn, B.H., Shaw, G.M., Korber, B.T., Bhattacharya, T., Perelson, A.S., 2009. Modeling sequence evolution in acute HIV-1 infection. J. Theor. Biol. 261, 341–360. http://dx.doi.org/10.1016/j.jtbi.2009.07.038.

Lewis, G.K., Fouts, T.R., Ibrahim, S., Taylor, B.M., Salkar, R., Guan, Y., Kamin-Lewis, R., Robinson, J.E., Devico, A.L., 2011. Identification and characterization of an immunogenic hybrid epitope formed by both HIV gp120 and human CD4 proteins. J. Virol. 85, 13097–13104. http://dx.doi.org/10.1128/JVI.05072-11.

Li, M., Gao, F., Mascola, J.R., Stamatatos, L., Polonis, V.R., Koutsoukos, M., Voss, G., Goepfert, P., Gilbert, P., Greene, K.M., Bilska, M., Kothe, D.L., Salazar-gonzalez, J.F., Wei, X., Decker, J.M., Hahn, B.H., Montefiori, D.C., 2005. Human immunodeficiency virus type 1 Env clones from acute and early subtype B infections for standardized assessments of vaccine-elicited neutralizing antibodies. J. Virol. 79, 10108–10125. http://dx.doi.org/10.1128/JVI.79.16.10108.

Li, M., Salazar-Gonzalez, J.F., Derdeyn, C.A., Morris, L., Williamson, C., Robinson, J.E., Decker, J.M., Li, Y., Salazar, M.G., Polonis, V.R., Mlisana, K., Karim, S.A., Hong, K., Greene, K.M., Bilska, M., Zhou, J., Allen, S., Chomba, E., Mulenga, J., Vwalika, C.,

Gao, D.C., Zhang, M., Korber, B.T.M., Hunter, E., Hahn, B.H., Montefiori, D.C., 2006. Genetic and neutralization properties of subtype C human immunodeficiency virus type 1 molecular env clones from acute and early heterosexually acquired infections in Southern Africa. J. Virol. 80, 11776–11790. http://dx.doi.org/10.1128/JVI.01730-06.

Liao, H., Guo, J., Lange, M.D., Fan, R., Zemlin, M., Su, K., Guan, Y., Zhang, Z., 2013. Contribution of VH replacement products to the generation of anti-HIV antibodies. Clin. Immunol. 146, 46–55. http://dx.doi.org/10.1016/j.clim.2012.11.003.

Liu, J., Bartesaghi, A., Borgnia, M.J., Sapiro, G., Subramaniam, S., 2008. Molecular architecture of native HIV-1 gp120 trimers. Nature 455, 109–113. http://dx.doi.org/10.1038/nature07159.

Lusso, P., Earl, P.L., Sironi, F., Santoro, F., Ripamonti, C., Scarlatti, G., Longhi, R., Berger, E.A., Burastero, S.E., 2005. Cryptic nature of a conserved, CD4-inducible V3 loop neutralization epitope in the native envelope glycoprotein oligomer of CCR5-restricted, but not CXCR4-using, primary human immunodeficiency virus type 1 strains. J. Virol. 79, 6957–6968. http://dx.doi.org/10.1128/JVI.79.11.6957-6968.2005.

Lyerly, H., Reed, D., Matthews, T., Langlois, A., Ahearne, P., Petteway, S., Weinhold, K., 1987. Anti-gp120 antibodies from HIV seropositive individuals mediate broadly reactive anti-HIV ADCC. AIDS Res. Hum. Retroviruses 3, 409–422.

Madhavi, V., Wren, L.H., Gonelli, C., Winnall, W.R., Parsons, M.S., Kramski, M., Kent, S.J., Stratov, I., 2014. Breadth of HIV-1 Env-specific antibody-dependent cellular cytotoxicity : relevance to global HIV vaccine design. AIDS 28, 1859–1870. http://dx.doi.org/10.1097/QAD.0000000000000310.

Maeda, K., Yoshimura, K., Shibayama, S., Habashita, H., Tada, H., Sagawa, K., Miyakawa, T., Aoki, M., Fukushima, D., Mitsuya, H., 2001. Novel low molecular weight spirodiketopiperazine derivatives potently inhibit R5 HIV-1 infection through their antagonistic effects on CCR5. J. Biol. Chem. 276, 35194–35200. http://dx.doi.org/10.1074/jbc.M105670200.

Marasco, W.A., Sui, J., 2007. The growth and potential of human antiviral monoclonal antibody therapeutics. Nat. Biotechnol. 25, 1421–1434. http://dx.doi.org/10.1038/nbt1363.

Mascola, J.R., Lewis, M.G., Stiegler, G., Vancott, T.C., Hayes, D., Louder, M.K., Brown, C.R., Sapan, C.V., Frankel, S.S., Lu, Y., Robb, M.L., Katinger, H., Birx, L., Harris, D., Cott, T.C.V.A.N., Birx, D.L., 1999. Protection of macaques against pathogenic simian/human immunodeficiency virus 89.6PD by passive transfer of neutralizing antibodies. J. Virol. 73, 4009–4018.

Mascola, J.R., Stiegler, G., VanCott, T.C., Katinger, H., Carpenter, C.B., Hanson, C.E., Beary, H., Hayes, D., Frankel, S.S., Birx, D.L., Lewis, M.G., 2000. Protection of macaques against vaginal transmission of a pathogenic HIV-1/SIV chimeric virus by passive infusion of neutralizing antibodies. Nat. Med 6, 207–210. http://dx.doi.org/10.1038/72318.

Matsushita, S., Robert-Guroff, M., Trepel, J., Cossman, J., Mitsuya, H., Broder, S., 1986. Human monoclonal antibody directed against an envelope glycoprotein of human T-cell leukemia virus type I. Proc. Natl. Acad. Sci. 83, 2672–2676.

Mbah, H.A., Burda, S., Gorny, M.K., Williams, C., Revesz, K., Zolla-Pazner, S., Nyambi, P.N., 2001. Effect of soluble CD4 on exposure of epitopes on primary, intact, native human immunodeficiency virus type 1 virions of different genetic clades. J. Virol. 75, 7785–7788. http://dx.doi.org/10.1128/JVI.75.16.7785-7788.2001.

McGuire, A.T., Glenn, J.A., Lippy, A., Stamatatos, L., 2014. Diverse recombinant HIV-1 Envs fail to activate B cells expressing the germline B cell receptors of the broadly neutralizing anti-HIV-1 antibodies PG9 and 447-52D. J. Virol. 88, 2645–2657. http://dx.doi.org/10.1128/JVI.03228-13.

Moldt, B., Rakasz, E.G., Schultz, N., Chan-Hui, P.-Y., Swiderek, K., Weisgrau, K.L., Piaskowski, S.M., Bergman, Z., Watkins, D.I., Poignard, P., Burton, D.R., 2012. Highly potent HIV-specific antibody neutralization in vitro translates into effective protection against mucosal SHIV challenge in vivo. Proc. Natl. Acad. Sci. U.S.A 109, 18921–18925. http://dx.doi.org/10.1073/pnas.1214785109.

Monde, K., Maeda, Y., Tanaka, Y., Harada, S., Yusa, K., 2007. Gp120 V3-dependent impairment of R5 HIV-1 infectivity due to virion-incorporated CCR5. J. Biol. Chem. 282, 36923–36932. http://dx.doi.org/10.1074/jbc.M705298200.

Montefiori, D.C., 2009. Measuring HIV neutralization in a luciferase reporter gene assay. In: Prasad, V., Kalpana, G. (Eds.), HIV Protocols SE-26, Methods In Molecular Biology™. Humana Press, pp. 395–405. http://dx.doi.org/10.1007/978-1-59745-170-3_26.

Montessori, V., Press, N., Harris, M., Akagi, L., Montaner, J.S.G., 2004. Adverse effects of antiretroviral therapy for HIV infection. CMAJ 170, 229–238.

Moore, J.P., Cao, Y., Ho, D.D., Koup, R.A., 1994. Development of the anti-gp120 antibody response during seroconversion to human immunodeficiency virus type 1. J. Virol. 68, 5142–5155.

Moulard, M., Phogat, S.K., Shu, Y., Labrijn, A.F., Xiao, X., Binley, J.M., Zhang, M.-Y., Sidorov, I.A., Broder, C.C., Robinson, J., Parren, P.W.H.I., Burton, D.R., Dimitrov, D.S., 2002. Broadly cross-reactive HIV-1-neutralizing human monoclonal Fab selected for binding to gp120-CD4-CCR5 complexes. Proc. Natl. Acad. Sci. U.S.A 99, 6913–6918. http://dx.doi.org/10.1073/pnas.102562599.

Nag, P., Kim, J., Sapiega, V., Landay, A.L., Bremer, J.W., Mestecky, J., Reichelderfer, P., Kovacs, A., Cohn, J., Weiser, B., Baum, L.L., 2004. Women with cervicovaginal antibody-dependent cell-mediated cytotoxicity have lower genital HIV-1 RNA loads. J. Infect. Dis. 190, 1970–1978. http://dx.doi.org/10.1086/425582.

Naik, E., Casanas, B., Pazare, A., Wabale, G., Sinnott, J., Salihu, H., 2009. Cost of treatment: the single biggest obstacle to HIV/AIDS treatment adherence in lower-middle class patients in Mumbai. India. Indian J. Sex. Transm. Dis. AIDS 30, 23–27. http://dx.doi.org/10.4103/0253-7184.55476.

Ng, C.T., Jaworski, J.P., Jayaraman, P., Sutton, W.F., Delio, P., Kuller, L., Anderson, D., Landucci, G., Richardson, B.a., Burton, D.R., Forthal, D.N., Haigwood, N.L., 2010. Passive neutralizing antibody controls SHIV viremia and enhances B cell

responses in infant macaques. Nat. Med. 16, 1117–1119. http://dx.doi.org/10.1038/nm.2233.

Nkolola, J.P., Bricault, C.a., Cheung, A., Shields, J., Perry, J., Kovacs, J.M., Giorgi, E., van Winsen, M., Apetri, A., Brinkman-van der Linden, E.C.M., Chen, B., Korber, B., Seaman, M.S., Barouch, D.H., 2014. Characterization and immunogenicity of a novel mosaic M HIV-1 gp140 trimer. J. Virol. 88, 9538–9552. http://dx.doi.org/10.1128/JVI.01739-14.

O'Doherty, U., Swiggard, W.J., Malim, M.H., 2000. Human immunodeficiency virus type 1 spinoculation enhances infection through virus binding. J. Virol. 74, 10074–10080. http://dx.doi.org/10.1128/JVI.74.21.10074-10080.2000.

Ochsenbauer, C., Edmonds, T.G., Ding, H., Keele, B.F., Decker, J., Salazar, M.G., Salazar-Gonzalez, J.F., Shattock, R., Haynes, B.F., Shaw, G.M., Hahn, B.H., Kappes, J.C., 2012. Generation of transmitted/founder HIV-1 infectious molecular clones and characterization of their replication capacity in CD4 T lymphocytes and monocyte-derived macrophages. J. Virol. 86, 2715–2728. http://dx.doi.org/10.1128/JVI.06157-11.

Overbaugh, J., Morris, L., 2012. The antibody response against HIV-1. Cold Spring Harb. Perspect. Med 2, a007039. http://dx.doi.org/10.1101/cshperspect.a007039.

Palmer, S., Maldarelli, F., Wiegand, A., Bernstein, B., Hanna, G.J., Brun, S.C., Kempf, D.J., Mellors, J.W., Coffin, J.M., King, M.S., 2008. Low-level viremia persists for at least 7 years in patients on suppressive antiretroviral therapy. Proc. Natl. Acad. Sci. U.S. A 105, 3879–3884. http://dx.doi.org/10.1073/pnas.0800050105.

Parren, P.W.H.I., Marx, P.A., Hessell, A.N.N.J., Harouse, J., Cheng-mayer, C., John, P., Burton, D.R., Luckay, A., Moore, J.P., 2001. Antibody protects macaques against vaginal challenge with a pathogenic R5 simian/human immunodeficiency virus at serum levels giving complete neutralization in vitro. J. Virol. 75, 8340–8347. http://dx.doi.org/10.1128/JVI.75.17.8340-8347.2001.

Platt, E.J., Wehrly, K., Kuhmann, S.E., Chesebro, B., Kabat, D., 1998. Effects of CCR5 and CD4 cell surface concentrations on infections by macrophagetropic isolates of human immunodeficiency virus type 1. J. Virol. 72, 2855–2864.

Pollara, J., Bonsignori, M., Moody, M.A., Liu, P., Alam, S.M., Hwang, K.-K., Gurley, T.C., Kozink, D.M., Armand, L.C., Marshall, D.J., Whitesides, J.F., Kaewkungwal, J., Nitayaphan, S., Pitisuttithum, P., Rerks-Ngarm, S., Robb, M.L., O'Connell, R.J., Kim, J.H., Michael, N.L., Montefiori, D.C., Tomaras, G.D., Liao, H.-X., Haynes, B.F., Ferrari, G., 2014. HIV-1 vaccine-induced C1 and V2 Env-specific antibodies synergize for increased antiviral activities. J. Virol. 88, 7715–7726. http://dx.doi.org/10.1128/JVI.00156-14.

Rader, C., Popkov, M., Neves, J.A., Barbas III, C.F., 2002. Integrin avb3-targeted therapy for Kaposi's sarcoma with an in vitro-evolved antibody. FASEB J. 10.1096/fj.02-0281fje.

Rerks-Ngarm, S., Pitisuttithum, P., Nitayaphan, S., Kaewkungwal, J., Chiu, J., Paris, R., Premsri, N., Namwat, C., de Souza, M., Adams, E., Benenson, M., Gurunathan, S., Tartaglia, J., McNeil, J.G., Francis, D.P., Stablein, D., Birx, D.L., Chunsuttiwat, S., Khamboonruang, C., Thongcharoen, P., Robb, M.L., Michael, N.L., Kunasol, P., Kim, J.H., 2009. Vaccination with ALVAC and AIDSVAX to prevent HIV-1 infection in Thailand. N. Engl. J. Med. 361, 2209–2220. http://dx.doi.org/10.1056/NEJMoa0908492.

Reust, C.E., 2011. Common adverse effects of antiretroviral therapy for HIV disease. Am. Fam. Phys. 83, 1443–1451.

Richman, D.D., Margolis, D.M., Delaney, M., Greene, W.C., Hazuda, D., Pomerantz, R.J., 2009. The challenge of finding a cure for HIV infection. Science 80, 1304–1307323, 1304–1307.

Roederer, M., Keele, B.F., Schmidt, S.D., Mason, R.D., Welles, H.C., Fischer, W., Labranche, C., Foulds, K.E., Louder, M.K., Yang, Z.-Y., Todd, J.-P.M., Buzby, A.P., Mach, L.V., Shen, L., Seaton, K.E., Ward, B.M., Bailer, R.T., Gottardo, R., Gu, W., Ferrari, G., Alam, S.M., Denny, T.N., Montefiori, D.C., Tomaras, G.D., Korber, B.T., Nason, M.C., Seder, R.A., Koup, R.A., Letvin, N.L., Rao, S.S., Nabel, G.J., Mascola, J.R., 2014. Immunological and virological mechanisms of vaccine-mediated protection against SIV and HIV. Nature 505, 502–508. http://dx.doi.org/10.1038/nature12893.

Salazar-Gonzalez, J.F., Bailes, E., Pham, K.T., Salazar, M.G., Guffey, M.B., Keele, B.F., Derdeyn, C.a., Farmer, P., Hunter, E., Allen, S., Manigart, O., Mulenga, J., Anderson, J.A., Swanstrom, R., Haynes, B.F., Athreya, G.S., Korber, B.T.M., Sharp, P.M., Shaw, G.M., Hahn, B.H., 2008. Deciphering human immunodeficiency virus type 1 transmission and early envelope diversification by single-genome amplification and sequencing. J. Virol. 82, 3952–3970. http://dx.doi.org/10.1128/JVI.02660-07.

Salazar-Gonzalez, J.F., Salazar, M.G., Keele, B.F., Learn, G.H., Giorgi, E.E., Li, H., Decker, J.M., Wang, S., Baalwa, J., Kraus, M.H., Parrish, N.F., Shaw, K.S., Guffey, M.B., Bar, K.J., Davis, K.L., Ochsenbauer-Jambor, C., Kappes, J.C., Saag, M.S., Cohen, M.S., Mulenga, J., Derdeyn, C.A., Allen, S., Hunter, E., Markowitz, M., Hraber, P., Perelson, A.S., Bhattacharya, T., Haynes, B.F., Korber, B.T., Hahn, B.H., Shaw, G.M., 2009. Genetic identity, biological phenotype, and evolutionary pathways of transmitted/founder viruses in acute and early HIV-1 infection. J. Exp. Med. 206, 1273–1289. http://dx.doi.org/10.1084/jem.20090378.

Sather, D.N., Armann, J., Ching, L.K., Mavrantoni, A., Sellhorn, G., Caldwell, Z., Yu, X., Wood, B., Self, S., Kalams, S., Stamatatos, L., 2009. Factors associated with the development of cross-reactive neutralizing antibodies during human immunodeficiency virus type 1 infection. J. Virol. 83, 757–769. http://dx.doi.org/10.1128/JVI.02036-08.

Scheid, J.F., Mouquet, H., Ueberheide, B., Diskin, R., Klein, F., Oliveira, T.Y.K., Pietzsch, J., Fenyo, D., Abadir, A., Velinzon, K., Hurley, A., Myung, S., Boulad, F., Poignard, P., Burton, D.R., Pereyra, F., Ho, D.D., Walker, B.D., Seaman, M.S., Bjorkman, P. J., Chait, B.T., Nussenzweig, M.C., 2011. Sequence and structural convergence of broad and potent HIV antibodies that mimic CD4 binding. Science 80, 1633–1637.

http://dx.doi.org/10.1126/science.1207227333, 1633–1637. http://dx.doi.org/10.1126/science.1207227.

Seaman, M.S., LeBlanc, D.F., Grandpre, L.E., Bartman, M.T., Montefiori, D.C., Letvin, N.L., Mascola, J.R., 2007. Standardized assesment of NAb responses elicited in rhesus monkeys immunized with single- or multi-clade HIV-1 envelope immunogens. Virology 367, 175–186.

Seaman, M.S., Xu, L., Beaudry, K., Kristi, L., Beddall, M.H., Miura, A., Sambor, A., Chakrabarti, B.K., Huang, Y., Bailer, R., Richard, A., Mascola, J.R., Nabel, G.J., Letvin, N.L., 2005. Multiclade human immunodeficiency virus type 1 envelope immunogens elicit broad cellular and humoral immunity in rhesus monkeys. J. Virol. 79, 2956–2963. http://dx.doi.org/10.1128/JVI.79.5.2956.

Shibata, R., Igarashi, T., Haigwood, N., Buckler-White, A., Ogert, R., Ross, W., Willey, R., Cho, M.W., Martin, M.A., 1999. Neutralizing antibody directed against the HIV-1 envelope glycoprotein can completely block HIV-1/SIV chimeric virus infections of macaque monkeys. Nat. Med 5, 204–210. http://dx.doi.org/10.1038/5568.

Simek, M.D., Rida, W., Priddy, F.H., Pung, P., Carrow, E., Laufer, D.S., Lehrman, J.K., Boaz, M., Tarragona-Fiol, T., Miiro, G., Birungi, J., Pozniak, A., McPhee, D.A., Manigart, O., Karita, E., Inwoley, A., Jaoko, W., DeHovitz, J., Bekker, L.-G., Pitisuttithum, P., Paris, R., Walker, L.M., Poignard, P., Wrin, T., Fast, P.E., Burton, D.R., Koff, W.C., 2009. Human immunodeficiency virus type 1 elite neutralizers: individuals with broad and potent neutralizing activity identified by using a high-throughput neutralization assay together with an analytical selection algorithm. J. Virol. 83 (7337–7348), http://dx.doi.org/10.1128/JVI.00110-09.

Smalls-Mantey, A., Doria-Rose, N., Klein, R., Patamawenu, A., Migueles, S.A., Ko, S.-Y., Hallahan, C.W., Wong, H., Liu, B., You, L., Scheid, J., Kappes, J.C., Ochsenbauer, C., Nabel, G.J., Mascola, J.R., Connors, M., 2012. Antibody-dependent cellular cytotoxicity against primary HIV-infected CD4+ T cells is directly associated with the magnitude of surface IgG binding. J. Virol. 86, 8672–8680. http://dx.doi.org/10.1128/JVI.00287-12.

Sok, D., Laserson, U., Laserson, J., Liu, Y., Vigneault, F., Julien, J.-P., Briney, B., Ramos, A., Saye, K.F., Le, K., Mahan, A., Wang, S., Kardar, M., Yaari, G., Walker, L.M., Simen, B.B., St. John, E.P., Chan-Hui, P.-Y., Swiderek, K., Kleinstein, S.H., Alter, G., Seaman, M.S., Chakraborty, A.K., Koller, D., Wilson, I.A., Church, G.M., Burton, D.R., Poignard, P., 2013. The effects of somatic hypermutation on neutralization and binding in the PGT121 family of broadly neutralizing HIV antibodies. PLoS Pathog 9, e1003754.

Stamatatos, L., Morris, L., Burton, D.R., Mascola, J.R., 2009. Neutralizing antibodies generated during natural HIV-1 infection: good news for an HIV-1 vaccine. Nat. Med. 15, 866–870. http://dx.doi.org/10.1038/nm.1949.

Takeuchi, Y., McClure, M.O., Pizzato, M., 2008. Identification of gammaretroviruses constitutively released from cell lines used for human immunodeficiency virus research. J. Virol. 82, 12585–12588. http://dx.doi.org/10.1128/JVI.01726-08.

Tamura, K., Peterson, D., Peterson, N., Stecher, G., Nei, M., Kumar, S., 2011. MEGA5: molecular evolutionary genetics analysis using maximum likelihood, evolutionary distance, and maximum parsimony methods. Mol. Biol. Evol. 28, 2731–2739. http://dx.doi.org/10.1093/molbev/msr121.

Thali, M., Moore, J.P., Furman, C., Charles, M., Ho, D.D., Robinson, J., Sodroski, J., 1993. Characterization of conserved human immunodeficiency virus type 1 gp120 neutralization epitopes exposed upon gp120-CD4 binding. J. Virol. 67, 3978–3988.

Trkola, A., Matthews, J., Gordon, C., Ketas, T., Moore, J.P., 1999. A cell line-based neutralization assay for primary human immunodeficiency virus type 1 isolates that use either the CCR5 or the CXCR4 coreceptor. J. Virol. 73, 8966–8974.

Veazey, R., Shattock, R.J., Pope, M., Kirijan, J.C., Jones, J., Qinxue, H., Ketas, T., Preston, M., Klasse, P.J., Burton, D.R., Moore, J.P., 2003. Prevention of virus transmission to macaque monkeys by a vaginally applied monoclonal antibody to HIV-1 gp120. Nat. Med. 9, 343–346. http://dx.doi.org/10.1038/nm.

Veillette, M., Désormeaux, A., Medjahed, H., Gharsallah, N.-E., Coutu, M., Baalwa, J., Guan, Y., Lewis, G., Ferrari, G., Hahn, B.H., Haynes, B.F., Robinson, J.E., Kaufmann, D.E., Bonsignori, M., Sodroski, J., Finzi, A., 2014. Interaction with cellular CD4 exposes HIV-1 envelope epitopes targeted by antibody-dependent cell-mediated cytotoxicity. J. Virol. 88, 2633–2644. http://dx.doi.org/10.1128/JVI.03230-13.

Walker, L.M., Huber, M., Doores, K.J., Falkowska, E., Pejchal, R., Julien, J.-P., Wang, S.-K., Ramos, A., Chan-Hui, P.-Y., Moyle, M., Mitcham, J.L., Hammond, P.W., Olsen, O.A., Phung, P., Fling, S., Wong, C.-H., Phogat, S., Wrin, T., Simek, M.D., Principal Investigators, P.G., Koff, W.C., Wilson, I.A., Burton, D.R., Poignard, P., 2011. Broad neutralization coverage of HIV by multiple highly potent antibodies. Nature 477, 466–470.

Walker, L.M., Phogat, S.K., Chan-Hui, P.-Y., Wagner, D., Phung, P., Goss, J.L., Wrin, T., Simek, M.D., Fling, S., Mitcham, J.L., Lehrman, J.K., Priddy, F.H., Olsen, O.a., Frey, S.M., Hammond, P.W., Kaminsky, S., Zamb, T., Moyle, M., Koff, W.C., Poignard, P., Burton,

D.R., 2009. Broad and potent neutralizing antibodies from an African donor reveal a new HIV-1 vaccine target. Science 80, 285–289. http://dx.doi.org/10.1126/science.1178746326, 285–289. http://dx.doi.org/10.1126/science.1178746.

Wei, X., Decker, J.M., Liu, H., Zhang, Z., Arani, R.B., Kilby, J.M., Saag, M.S., Wu, X., Shaw, G.M., Kappes, J.C., 2002. Emergence of resistant human immunodeficiency virus type 1 in patients receiving fusion inhibitor (T-20) monotherapy. Antimicrob. Agents Chemother. 46, 1896–1905. http://dx.doi.org/10.1128/AAC.46.6.1896.

Wren, L., Parsons, M.S., Isitman, G., Center, R.J., Kelleher, A.D., Stratov, I., Bernard, N.F., Kent, S.J., 2012. Influence of cytokines on HIV-specific antibody-dependent cellular cytotoxicity activation profile of natural killer cells. PLoS One 7, e38580.

Wren, L.H., Chung, A.W., Isitman, G., Kelleher, A.D., Parsons, M.S., Amin, J., Cooper, D.A., Stratov, I., Navis, M., Kent, S.J., 2013. Specific antibody-dependent cellular cytotoxicity responses associated with slow progression of HIV infection. Immunology 138, 116–123. http://dx.doi.org/10.1111/imm.12016.

Wu, X., Sambor, A., Nason, M.C., Yang, Z.-Y., Wu, L., Zolla-Pazner, S., Nabel, G.J., Mascola, J.R., 2008. Soluble CD4 broadens neutralization of V3-directed monoclonal antibodies and guinea pig vaccine sera against HIV-1 subtype B and C reference viruses. Virology 380, 285–295. http://dx.doi.org/10.1016/j.virol.2008.07.007.

Wu, X., Zhou, T., Zhu, J., Zhang, B., Georgiev, I., Wang, C., Chen, X., Longo, N.S., Louder, M., McKee, K., O'Dell, S., Perfetto, S., Schmidt, S.D., Shi, W., Wu, L., Yang, Y., Yang, Z.-Y.Z., Zhang, Z., Bonsignori, M., Crump, J.A., Kapiga, S.H., Sam, N.E., Haynes, B.F., Simek, M., Burton, D.R., Koff, W.C., Doria-Rose, N.A., Connors, M., Program, N.C.S., Mullikin, J.C., Nabel, G.J., Roederer, M., Shapiro, L., Kwong, P.D., Mascola, J.R., O'Dell, S., 2011. Focused evolution of HIV-1 neutralizing antibodies revealed by structures and deep sequencing. Science 333, 1593–1602. http://dx.doi.org/10.1126/science.1207532.

Xiang, S., Doka, N., Choudhary, R.K., Sodroski, J., Robinson, J.E., 2002. Characterization of CD4-induced epitopes on the HIV type 1 gp120 envelope glycoprotein recognized by neutralizing human monoclonal antibodies. AIDS Res. Hum. Retroviruses 18, 1207–1217.

Xiao, P., Zhao, J., Patterson, L.J., Brocca-Cofano, E., Venzon, D., Kozlowski, P.A., Hidajat, R., Demberg, T., Robert-Guroff, M., 2010. Multiple vaccine-elicited nonneutralizing antienvelope antibody activities contribute to protective efficacy by reducing both acute and chronic viremia following simian/human immunodeficiency virus SHIV89.6P challenge in rhesus macaques. J. Virol. 84, 7161–7173. http://dx.doi.org/10.1128/JVI.00410-10.

Xiao, X., Chen, W., Feng, Y., Zhu, Z., Prabakaran, P., Wang, Y., Zhang, M.-Y., Longo, N.S., Dimitrov, D.S., 2009. Germline-like predecessors of broadly neutralizing antibodies lack measurable binding to HIV-1 envelope glycoproteins: implications for evasion of immune responses and design of vaccine immunogens. Biochem. Biophys. Res. Commun. 390, 404–409. http://dx.doi.org/10.1016/j.bbrc.2009.09.029.

Yoshimura, K., Shibata, J., Kimura, T., Honda, A., Maeda, Y., Koito, A., Murakami, T., Mitsuya, H., Matsushita, S., 2006. Resistance profile of a neutralizing anti-HIV monoclonal antibody, KD-247, that shows favourable synergism with anti-CCR5 inhibitors. AIDS 20, 2065–2073. http://dx.doi.org/10.1097/01.aids.0000247587.31320.fe.

Zhou, T., Georgiev, I., Wu, X., Yang, Z.-Y., Dai, K., Finzi, A., Do Kwon, Y., Scheid, J.F., Shi, W., Xu, L., Yang, Y., Zhu, J., Nussenzweig, M.C., Sodroski, J., Shapiro, L., Nabel, G.J., Mascola, J.R., Kwong, P.D., 2010. Structural basis for broad and potent neutralization of HIV-1 by antibody VRC01. Science 329, 811–817. http://dx.doi.org/10.1126/science.1192819.

Zhu, J., Wu, X., Zhang, B., McKee, K., O'Dell, S., Soto, C., Zhou, T., Casazza, J.P., Program, N.C.S., Mullikin, J.C., Kwong, P.D., Mascola, J.R., Shapiro, L., 2013. De novo identification of VRC01 class HIV-1–neutralizing antibodies by next-generation sequencing of B-cell transcripts. Proc. Natl. Acad. Sci. 110, E4088–E4097. http://dx.doi.org/10.1073/pnas.1306262110.

Zolla-Pazner, S., 2004. Identifying epitopes of HIV-1 that induce protective antibodies. Nat. Rev. Immunol. 4, 199–210. http://dx.doi.org/10.1038/nri1307.

Zolla-Pazner, S., 2014. A critical question for HIV vaccine development: which antibodies to induce. Science 80, 167–168. http://dx.doi.org/10.1126/science.1256526345, 167–168. http://dx.doi.org/10.1126/science.1256526.

Zolla-Pazner, S., Kong, X.-P., Jiang, X., Cardozo, T., Nádas, A., Cohen, S., Totrov, M., Seaman, M.S., Wang, S., Lu, S., 2011. Cross-clade HIV-1 neutralizing antibodies induced with V3-scaffold protein immunogens following priming with gp120 DNA. J. Virol. 85, 9887–9898. http://dx.doi.org/10.1128/JVI.05086-11.

Zuo, T., Shi, X., Liu, Z., Guo, L., Zhao, Q., Guan, T., Pan, X., Jia, N., Cao, W., Zhou, B., Goldin, M., Zhang, L., 2011. Comprehensive analysis of pathogen-specific antibody response in vivo based on an antigen library displayed on surface of yeast. J. Biol. Chem. 286, 33511–33519. http://dx.doi.org/10.1074/jbc.M111.270553.

Structural basis of clade-specific HIV-1 neutralization by humanized anti-V3 monoclonal antibody KD-247

Karen A. Kirby,[*,†,1] Yee Tsuey Ong,[*,†,1] Atsuko Hachiya,[*,†] Thomas G. Laughlin,[*,†] Leslie A. Chiang,[*,†] Yun Pan,[*,†] Jennifer L. Moran,[*,†] Bruno Marchand,[*,†] Kamalendra Singh,[*,†] Fabio Gallazzi,[‡] Thomas P. Quinn,[§] Kazuhisa Yoshimura,[¶] Toshio Murakami,[‖] Shuzo Matsushita,[#] and Stefan G. Sarafianos[*,†,§,2]

*Christopher S. Bond Life Sciences Center, †Department of Molecular Microbiology and Immunology, School of Medicine, ‡Structural Biology Core, and §Department of Biochemistry, University of Missouri, Columbia, Missouri, USA; ¶AIDS Research Center, National Institute of Infectious Diseases, Tokyo, Japan; ‖The Chemo-Sero-Therapeutic Research Institute (Kaketsuken), Kyokushi, Kikuchi, Kumamoto, Japan; and #Division of Clinical Retrovirology and Infectious Diseases, Center for AIDS Research, Kumamoto University, Kumamoto, Japan

ABSTRACT Humanized monoclonal antibody KD-247 targets the Gly^{312}-Pro^{313}-Gly^{314}-Arg^{315} arch of the third hypervariable (V3) loop of the HIV-1 surface glycoprotein. It potently neutralizes many HIV-1 clade B isolates, but not of other clades. To understand the molecular basis of this specificity, we solved a high-resolution (1.55 Å) crystal structure of the KD-247 antigen binding fragment and examined the potential interactions with various V3 loop targets. Unlike most antibodies, KD-247 appears to interact with its target primarily through light chain residues. Several of these interactions involve Arg^{315} of the V3 loop. To evaluate the role of light chain residues in the recognition of the V3 loop, we generated 20 variants of KD-247 single-chain variable fragments with mutations in the antigen-binding site. Purified proteins were assessed for V3 loop binding using Alpha-Screen technology and for HIV-1 neutralization. Our data revealed that recognition of the clade-specificity defining residue Arg^{315} of the V3 loop is based on a network of interactions that involve Tyr^{L32}, Tyr^{L92}, and Asn^{L27d} that directly interact with Arg^{315}, thus elucidating the molecular interactions of KD-247 with its V3 loop target.—Kirby, K. A., Ong, Y. T., Hachiya, A., Laughlin, T. G., Chiang, L. A., Pan, Y., Moran, J. L., Marchand, B., Singh, K., Gallazzi, F., Quinn, T. P., Yoshimura, K., Murakami, T., Matsushita, S., Sarafianos, S. G. Structural basis of clade-specific HIV-1 neutralization by humanized anti-V3 monoclonal antibody KD-247. *FASEB J.* 29, 70–80 (2015). www.fasebj.org

Key Words: crystal structure · entry · HIV · single-chain variable fragment

ALTHOUGH THE AVAILABILITY of highly active antiretroviral therapy (HAART) has significantly reduced the rate of

HIV-1-related deaths (1), the development of a vaccine against multiple HIV-1 clades remains a challenge. The extensive glycosylation of the envelope glycoprotein (Env) (2) and the shedding of Env from the virus surface (3) are two of several mechanisms by which HIV-1 escapes the host immune system. Although most of the neutralizing antibodies elicited after HIV-1 infection are clade specific (4), some are broadly neutralizing, including b12 (5), 2G12 (6), 4E10 (7), 2F5 (8), PG9 and PG16 (9), VRC01 and VRC02 (10), PGT121-145 (11), NIH45-46 (12), and 10E8 (13).

HIV-1 Env comprises the noncovalently associated gp120 and gp41, which are proteolytic cleavage products of the gp160 precursor (14). The third hypervariable (V3) loop of gp120 that interacts with the CCR5 or CXCR4 coreceptor during HIV-1 entry (15) is one of the most immunodominant regions of HIV-1 (16–18). V3 loops of different HIV-1 strains and clades are highly variable in sequence and structural conformation (19). Anti-V3 antibodies elicited from animal immunization studies are generally clade-specific and show little or no cross-reactivity (19). Nevertheless, several anti-V3 antibodies, such as 447-52D, 2219, F425-B4e8, 2557, and 3074, have been reported to show cross-reactivity against a panel of HIV-1 isolates from various clades (20–25). The recent discovery of broadly neutralizing V3-targeting PGT121 and PGT128 antibodies continues to shed light on V3 loop immunogen design (26).

KD-247 is a humanized version of the C25 murine monoclonal antibody (mAb), which was isolated from the sequential immunization of mice with clade B HIV-1 V3 loop peptides (27). KD-247 can neutralize a broad

---

Abbreviations: CD, circular dichroism; CDR, complementarity determining region; Env, envelope glycoprotein; Fab, antigen-binding fragment; GPGR, Gly^{312}-Pro^{313}-Gly^{314}-Arg^{315}; mAb, monoclonal antibody; scFv, single-chain variable fragment; V3 loop, third hypervariable loop

spectrum of CCR5- and CXCR4-tropic viruses and HIV-1 quasi-species from patient plasma and peripheral blood mononuclear cells (27, 28). Passive transfer of KD-247 in simian/human immunodeficiency virus–infected monkeys protected the animals against CD4$^+$ T cell loss and increase of virus load (29, 30). This suggests that KD-247 can serve as a potential immunotherapy component in treating HIV-1-infected patients. Therefore, a structural understanding of the KD-247–V3 interactions should help us design strategies for expanding the clade specificity of this antibody.

The minimum V3 sequence required for KD-247 binding was mapped to Ile^{309}-Gly^{312}-Pro^{313}-Gly^{314}-Arg^{315} (IGPGR) at the V3 arch, and Arg^{315} is crucial for the interaction with KD-247 (27). We hypothesized that the interactions of KD-247 with residue 315 of the V3 loop strongly affect the clade specificity of KD-247, which can efficiently neutralize clade B viruses with Arg^{315} at the V3 arch, but not viruses from other clades that have a Gln^{315} (e.g., Gly^{312}-Pro^{313}-Gly^{314}-Gln^{315} in most non–clade B viruses).

To understand the molecular basis of KD-247 clade specificity, we have solved the crystal structure of its unliganded antigen binding fragment (Fab) and used it in molecular modeling studies with V3 peptides to obtain insights into possible binding interactions between the Fab and the target V3 loop. The proposed interactions were validated by site-specific mutagenesis of single-chain variable fragment (scFv) KD-247 variants, peptide binding assays, and cell-based HIV-1 neutralization assays.

MATERIALS AND METHODS

Fab production and purification

KD-247 was obtained from the Chemo-Sero-Therapeutic Research Institute (27). Fab was prepared by digesting KD-247 (34°C, 7 h) with 0.2 mg of papain agarose (Sigma-Aldrich, St. Louis, MO, USA) per milligram of antibody at 2 mg/ml in sodium acetate pH 5.5, 50 mM L-cysteine and 1 mM EDTA. The reaction was stopped by removing the papain agarose using a 0.22 μm filter. Digested Fab was purified with a HiTrap SP HP 5 ml column (GE Healthcare, Piscataway, NJ, USA) using sodium acetate pH 5.5 as the binding buffer and sodium acetate pH 5.5, 1 M NaCl, as the elution buffer.

Crystallization and data collection

KD-247 Fab crystals were grown in sitting drop trays. Drops containing 1 μl Fab (10 mg/ml) and 1 μl well solution were allowed to equilibrate with 0.5 ml 1.9 M ammonium sulfate/0.05 M sodium acetate pH 4.4 at 21°C. Octahedral-shaped crystals appeared after 3 d and cryoprotected with 20% glycerol. Data were processed to 1.55 Å using d*TREK (31), and indexed in P2$_1$2$_1$2$_1$ (a = 61.1 Å, b = 69.2 Å, and c = 111.8 Å) with one Fab per asymmetric unit. The Matthews coefficient (32) was 2.5 Å^3/Da (solvent content ~51%).

Structure determination and refinement

The structure was determined by molecular replacement MOLREP (33). The Fab variable and constant domains of

1T3F from the Protein Data Bank (PDB) were treated as separate search models. After initial rigid-body and restrained refinement in Phenix (34), R$_{work}$ dropped to 0.3377, with an R$_{free}$ of 0.3560. Simulated annealing was used to remove model bias. An initial model was built using ARP/wARP (35) with refinement using Refmac (36). Several cycles of model building and refinement were carried out using Coot (37) and Phenix (Table 1). Final atomic coordinates and structure factors have been deposited (PDB ID: 3NTC).

Superposition analysis

The coordinates of several Fab–V3 peptide complexes were downloaded from the PDB: 1ACY, 1AI1, 1F58, 1GGI, 1NAK, 1Q1J, 2B0S, 2QSC, and 3MLW. These complexes were chosen specifically because all have V3 peptides based on the HIV-1$_{MN}$ sequence, which is efficiently neutralized by KD-247. The Fab portions were aligned with the KD-247 Fab in Coot using the light chain for alignment. Upon each alignment, the position of the V3 peptide with respect to the KD-247 complementarity determining region (CDR) was visually inspected. The V3 peptide that fit best in the KD-247 binding pocket

TABLE 1. *Data collection and refinement statistics*

Data collection	Value
Wavelength (Å)	1.07
Resolution (Å)	1.55 (1.61–1.55)^a
Space group	P2$_1$2$_1$2$_1$
Cell dimensions	
a (Å)	61.1
b (Å)	69.2
c (Å)	111.8
Observed reflections	448,730
Unique reflections	68,709
Redundancy	6.5 (4.4)
Completeness (%)	99.0 (92.0)
R$_{sym}$^{b}	0.068 (0.595)
Avg I/σ	10.2 (1.6)
Refinement statistics for all reflections >0.0 σ F	
Resolution (Å)	19.75–1.55
No. of reflections (working)	68,481
No. of reflections (test)	2,748
R$_{work}$^{c}	0.1901
R$_{free}$^{d}	0.2099
No. of Fab atoms	3365
No. of water molecules	575
No. of solvent molecules	30
Overall B value (Å^2)	
Fab	26.28
Solvents	39.54
Wilson B value (Å^2)	24.16
Ramachandran plot (%)^e	
Favored	98.2
Allowed	1.8
Disallowed	0.0
RMSD bond length (Å)	0.004
RMSD angle (°)	0.992

^{a}Values in parentheses are for the outer resolution shell. ^{b}R$_{sym}$ = Σ$_{hkl}$ |I − < I >| / Σ$_{hkl}$ |I|. ^{c}R$_{cryst}$ = Σ$_{hkl}$ |F$_{obs}$ − F$_{calc}$| / Σ$_{hkl}$ |F$_{obs}$|. ^{d}R$_{free}$ = R$_{cryst}$, except 4% of the data excluded from the refinement. ^{e}Evaluated by MolProbity (48).

was from 2QSC (RP142 V3). The V3 peptide from the aligned 2QSC coordinates was removed and loaded with KD-247 into SYBYL (7.3.5; Tripos, St. Louis, MO, USA) and taken through a slight minimization procedure to reduce minor steric interactions.

Modeling of G314E and R315K KD-247-resistant V3 peptides with KD-247

Models of the G314E and R315K V3 peptides were generated by performing a simple mutation of the aligned and minimized RP142 peptide used in the superposition analysis at the 314 and 315 positions. All possible rotamers of Glu^{314} and Lys^{315} demonstrated steric clashes with KD-247 CDR residues.

Preparation of KD-247 scFv variants

Single amino acid substitutions of Asn^{L27d}, Tyr^{L32}, and Tyr^{L92} in the background pET28a3c-KD247 scFv (38) were generated by site-directed mutagenesis and verified by DNA sequencing. scFv variants were expressed in BL21(DE3) *Escherichia coli* and purified as previously described (38). scFv in the inclusion bodies was denatured and refolded before purification on HisTrap and HiPrep 26/60 Sephacryl S200 HR columns (GE Healthcare, Piscataway, NJ, USA). The secondary structure of the refolded scFv was examined using far-UV circular dichroism (CD) spectroscopy as previously described (38). Data were collected on a J-815 CD Spectrometer (JASCO, Easton, MD, USA) at 0.2 mg/ml from 190 to 240 nm. CD spectra were plotted using GraphPad Prism 5 (GraphPad Software Inc., La Jolla, CA, USA). CD spectra were analyzed by the SELCON3 (39, 40) and K2D3 (41) methods using the DichroWeb online analysis software (42, 43). Reference data sets 4 and 7 (range 190–240 nm) were used in the analyses (44).

V3 peptide binding assay

Biotinylated clade B V3 peptide was synthesized at the Structural Biology Core (University of Missouri, Columbia, MO, USA). The sequence (Biotin-GCRKRIHIGPGRAFYTC) was derived from MN V3 loop sequence (304–309, 312–319 based on HXB2 numbering). Peptide binding assays were performed in 96-well ½ area white plates (Perkin Elmer, Waltham, MA, USA) using a 40 μl reaction volume containing donor and acceptor beads (final concentration 20 μg/ml), 1× phosphate-buffered saline (PBS) pH 7.4, 0.01% Tween-20, and 0.1 mg/ml bovine serum albumin. A total of 200 nM N-terminal 6× histidine (His6)-tagged scFv variants (50 nM final) were incubated with 400 nM biotinylated V3 peptide (100 nM final) for 1 h at room temperature. A total of 80 μg/ml of nickel chelated acceptor beads (Perkin Elmer, Waltham, MA, USA) were added to the wells and allowed to incubate for another hour in the dark before adding 80 μg/ml of streptavidin-coated donor beads (Perkin Elmer, Waltham, MA, USA). After 30 min incubation in the dark, the plates were analyzed using an EnSpire Plate Reader (Perkin Elmer, Waltham, MA, USA). Parental KD-247 scFv (wild-type, WT) was the positive control that gives high signal counts because of its strong binding to the clade B V3 peptide. A reaction containing only the peptide but no scFv served as the negative control. The signals of all the scFv variants were compared to the WT scFv signal. Statistical analyses were performed using 2-tailed 1-sample *t* test and Wilcoxon signed rank test at 95% confidence.

HIV-1 neutralization assay

Maraviroc, TZM-bl cells (from Dr. John C. Kappes, Dr. Xiaoyun Wu, and Tranzyme Inc., Durham, NC, USA), pSG3ΔEnv (from Drs. John C. Kappes and Xiaoyun Wu), pWT/BaL plasmid (Dr. Bryan Cullen), and H9/HTLV-III$_{MN}$ NIH 1984 (Dr. Robert Gallo) were obtained through the U.S. NIH AIDS Reagent Program. The plasmid for expression of JR-FL Env (pCXN-JR-FL-Env) was from Dr. Shuzo Matsushita. TZM-bl cells were maintained in Dulbecco's modified Eagle's medium (DMEM) supplemented with 10% heat-inactivated fetal bovine serum (FBS), 100 units/ml penicillin, and 100 μg/ml streptomycin. The 293T cells were maintained in DMEM supplemented with 10% FBS, and penicillin/streptomycin. H9/HTLV-III$_{MN}$ NIH 1984 was passaged in RPMI 1640 supplemented with L-glutamine and 10% FBS.

Replication-competent HIV-1$_{BaL}$ and replication-deficient pseudotyped HIV-1 were produced by 293T transfection with pWT/BaL or pSG3ΔEnv and pCXN-JR-FL-Env plasmids (38). Replication-competent HIV-1$_{MN}$ was obtained from supernatant of H9/HTLV-III$_{MN}$ NIH 1984 culture (45, 46). Virus titers were determined using the previously described 50% tissue culture infectious dose (TCID$_{50}$) assay (47).The ability of KD-247 scFv variants to neutralize JR-FL Env pseudotyped HIV-1 was first evaluated. A total of 100 TCID$_{50}$ pseudotyped virus was preincubated with scFv variants (5 μM final concentration) (37°C) for 1 h before infecting TZM-bl cells (preseeded 1 × 10^4 cells/well). A total of 10 nM maraviroc (targets CCR5) was used as a positive control. Luciferase activity of infected TZM-bl cells was determined at 48 h postinfection using Bright-Glo Reagent (Promega, Madison, WI, USA). The relative infectivity was determined as ratio of the relative light units in the presence of scFv to virus control (PBS treated). The percentage of neutralization was calculated as 100 × (1 − relative infectivity). scFv variants that showed more than 50% neutralization were further studied as described above using HIV-1$_{BaL}$ or HIV-1$_{MN}$ in the presence of scFv at various concentrations to determine 50% neutralization concentration (EC$_{50}$). Data from at least three independent experiments were plotted using nonlinear regression equations in GraphPad Prism 5 software to obtain EC$_{50}$ values.

RESULTS

KD-247 Fab crystal structure

The KD-247 Fab structure was determined to 1.55 Å, the highest resolution reported for any apo humanized antibody (**Fig. 1A**). It was refined to an R-factor of 19% and an R$_{free}$ of 21%. More than 98% of the KD-247 Fab residues had main chain torsion angles in the energetically favored regions of the Ramachandran plot (48), with no residues in disallowed regions (49) (Table 1). Using RBOW, the elbow angle of the KD-247 Fab was determined to be 127°, which falls within the range commonly observed for Fabs with κ light chains (50).

KD-247 is the first humanized anti-V3 mAb to be structurally characterized. The heavy and light chains were numbered using the Kabat numbering system (51, 52). The heavy and light chains are designated with an "H" and an "L", respectively. The CDR loops L1, L2, L3, H1, and H2 belong to canonical classes κ-3, 1, κ-1, 1, and 1 (53). The CDR H3 loop exhibits a kinked base conformation with the observation of the conserved hydrogen bond between the ring nitrogen of Trp^{H103}
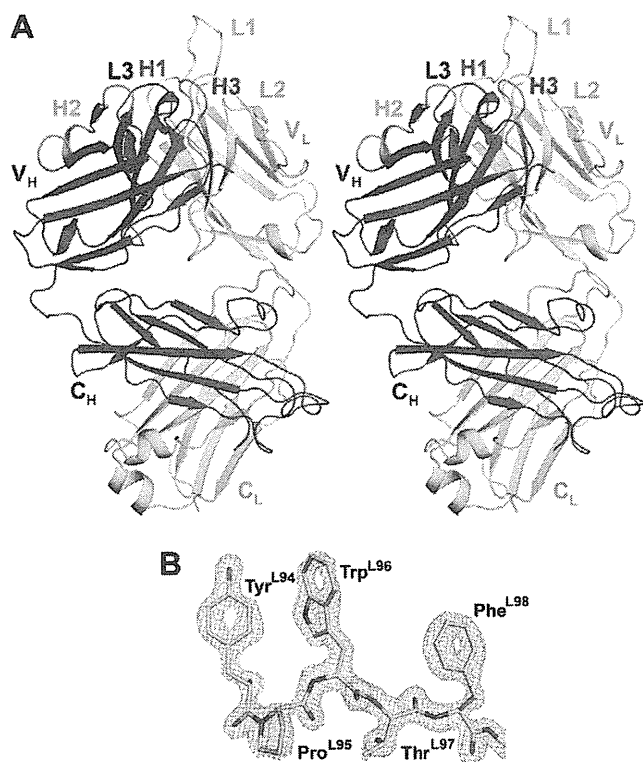
A

B

Figure 1. Crystal structure of KD-247 Fab. (A) Stereo view of the Fab including CDR regions (L1, cyan; L2, green; L3, blue; H1, red; H2, orange; H3, purple). Light and heavy chains are shown in light and dark gray. (B) $3Fo-2Fc$ electron density map of light chain residues ($\sigma = 2.0$). All structural images were generated using PyMOL (http://www.pymol.org/).

and the carbonyl oxygen of Met^{H100A}; there is no salt bridge between Arg^{H94} and Asp^{H101} (54). Excellent electron density was continuous almost throughout the entire molecule (Fig. 1B), allowing assignment of partial occupancy and alternate conformations. Slightly disordered loops were observed for residues 42–43, 64–66, and 101–102 in the heavy chain but were included in the model.

The KD-247 Fab CDR L1 loop is very similar to the L1 loop from other Fabs, including the Fab of nonneutralizing HIV-1 antibody 13H11 (PDB ID: 3MNV; light chain RMSD compared to KD-247 light chain [$RMSD_L$] determined by PDBeFold = 0.62 Å), the Fab of a mAb that neutralizes human rhinovirus serotype 2 (PDB ID: 1BBD; $RMSD_L$ = 0.73 Å), an antitumor CH2-domain-deleted humanized antibody (PDB ID: 1ZA6; $RMSD_L$ = 0.55 Å), the Fab of human germ-line antibody 1-69/B3 (PDB ID: 3QOT; $RMSD_L$ = 0.44 Å), and the Fab of *Mus musculus* germ-line antibody S25-2 (PDB ID: 1Q9K; $RMSD_L$ = 0.65 Å) (Fig. 2A). The CDR L1 loop is considerably longer in the KD-247 Fab (17 residues long) than what is observed for other anti-V3 loop antibodies, including murine antibody 83.1 (PDB ID: 1NAK) and human antibodies F425-B4e8 (2QSC), 2219 (2B0S), and 1006-15D (3MLW) (Fig. 2B). The CDR L1 loop of anti-V3 loop murine antibody 83.1 (PDB ID: 1NAK) is 16 residues long but is bent in the crystal structure to avoid

crystal packing clashes with residues from the variable heavy chain of a symmetry-related molecule (55).

We pursued cocrystallization of the KD-247 Fab in complex with various V3 peptides of different sequences and lengths, which resulted in many beautiful crystals but poor X-ray diffraction or internal lattice problems that could not be resolved. The crystal packing of the apo Fab does not allow room for the peptide to bind through soaking experiments. Thus, we constructed a molecular model of the KD-247 Fab in complex with the V3 loop in order to understand the molecular details of HIV-1 clade B V3 loop recognition by KD-247.

Superposition of the V3 loop

In our model of the KD-247 Fab crystal structure in complex with a clade B V3 $Gly^{312}-Pro^{313}-Gly^{314}-Arg^{315}$ (GPGR)-containing peptide, the V3 residues are designated with a "P" and numbered according to the HXB2 sequence (56). We aligned previously determined Fab-V3 complexes to KD-247 Fab. The V3 peptides of many Fab-V3 complexes that aligned with the KD-247 Fab did not fit well after superposition with the KD-247 binding pocket. One exception was the V3 peptide from 2QSC, derived from MN and called RP142 ($Y^{P301}NKRKRIHI^{P309}$ $G^{P312}PGRAFYTTKNIIGC^{P326}$) (57, 58).

The RP142 peptide fits nicely into the binding pocket, with only minor obstructions. The side chains of Ile^{P309} and Tyr^{P318} and the main chain of Phe^{P317} in V3 were in close contact (<2.0 Å) with the Trp^{H33}, Asn^{H58}, and Tyr^{L94} side chains of KD-247 Fab. After minimization, the positions of the important GPGR residues were virtually unchanged. The primary interactions between the RP142 peptide and the KD-247 Fab involve the V3 arch of the loop and the CDR L1 and L3 regions (Fig. 2C). Previous studies have shown that the characteristic observed interactions between anti-V3 Fabs with the V3 peptides occur in the long extended CDR H3 (59–61). In our case and in the 2QSC structure, Arg^{315} of the V3 loop interacts with light chain Fab residues. The most interesting interaction occurs between Arg^{315} of the RP142 peptide and KD-247 Tyr^{L32} and Tyr^{L92} (Fig. 2D). Arg^{315} appears to be stabilized by van der Waals interactions with the side chains of the two tyrosines and additionally by a hydrogen bond with the phenoxy group of Tyr^{L92}. The arginine is also further stabilized by a hydrogen bond with Asn^{L27d}. An intricate hydrogen bond network between CDR L1 loop residues Tyr^{L32}, Asp^{L28}, and Asn^{L27d} helps to stabilize Tyr^{L32} and Asn^{L27d} in positions to interact with Arg^{315} (Fig. 2D).

G314E and R315K KD-247-resistant V3 peptides with KD-247

Two mutations in the V3 arch confer KD-247 resistance. HIV-1$_{JR-FL}$ with G314E was neutralized 16-fold less efficiently by KD-247 than HIV-1$_{JR-FL}$ without this mutation (62). An HIV-1$_{BaL}$ variant containing a potential N-linked glycosylation site (PNGS) insertion in V2 and an R315K mutation in the V3 arch provided a very high resistance phenotype to KD-247 (63). The long Glu

Figure 2. Structural comparison of KD-247 with other Fabs and potential interactions with a V3 peptide. (A) Similarities of the KD-247 CDR L1 loop (cyan) to other Fabs (PDB ID: 3MNV, red; 1BBD, orange; 1ZA6, green; 3QOT, magenta; 1Q9K, blue). The RMSD between the light chain of all Fabs and KD-247 is <0.75 Å. (B) The KD-247 CDR L1 loop (cyan) is unique from other anti-V3 mAbs (PDB ID: 1NAK, yellow; 2QSC, gray; 2B0S, pink; 3MLW, brown). (C) Stereo view of KD-247 (surface representation, colors as in Fig. 1) with the RP142 peptide (white cartoon/yellow sticks) modeled in the binding pocket. (D) Interactions between Arg^{315} of the RP142 peptide, Tyr^{L32} and Asn^{L27d} of CDR L1 (cyan) and Tyr^{L92} of CDR L3 (blue; dashed lines are H bonds). Tyr^{L32} is stabilized by an H-bond network that includes Asp^{L28} and Asn^{L27d} of CDR L1.
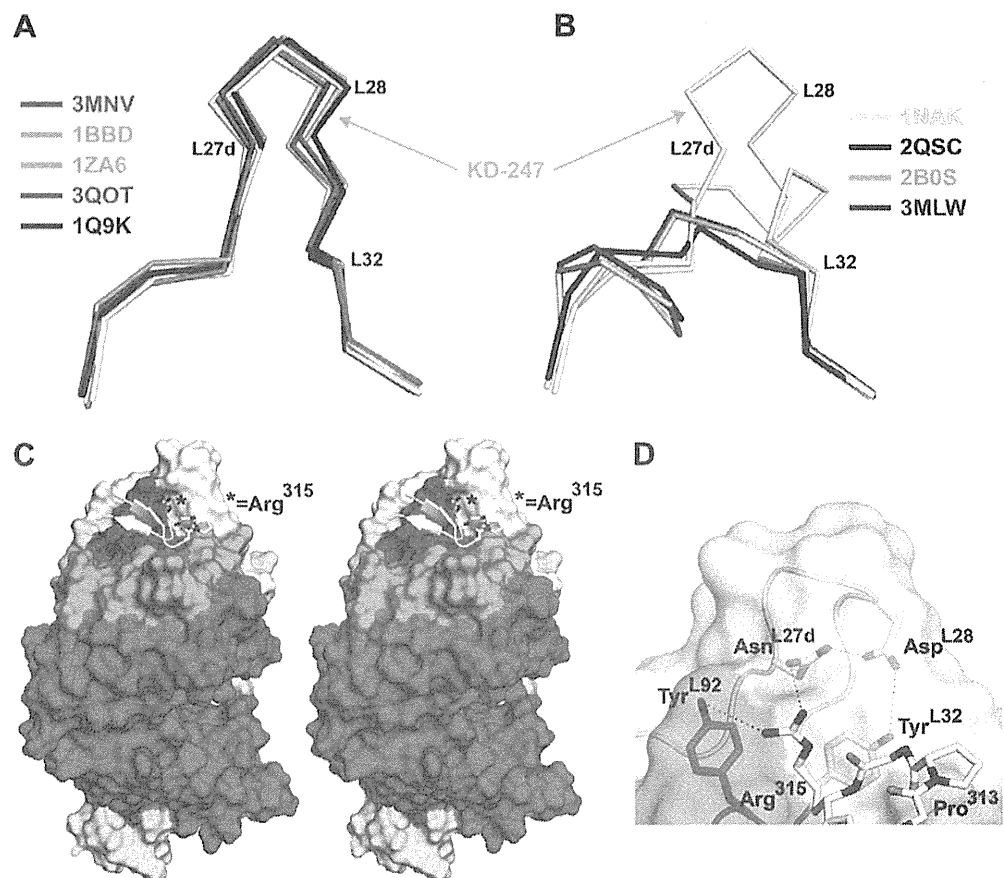
chain in G314E V3 causes steric clashes with KD-247 CDR L1, L2, and H3 (data not shown). Similarly, R315K also creates steric clashes with CDR L1 and L3 of KD-247.

KD-247 scFv variants

On the basis of our KD-247 structure-guided model, we designed KD-247 variants in a smaller size 30 kDa scFv antibody format. scFv variants with single or double Ala substitutions at Asn^{L27d}, Tyr^{L32}, and/or Tyr^{L92} were generated to disrupt the proposed interactions. To understand the proposed interactions of Tyr^{L32} and Tyr^{L92} with Arg^{315}, we generated scFv variants with Phe substitutions at these positions. Additional substitutions at Asn^{L27d}, Tyr^{L32}, and Tyr^{L92} were generated to further understand the effects of side chains on the KD-247 interactions with the GPGR V3 arch. We proposed that substitution with polar side chain of Asn or Gln at Asn^{L27d}, Tyr^{L32}, and Tyr^{L92} will maintain affinity for Arg^{315}. Substitution with the long basic side chain of Arg and Lys or the short acidic side chain of Asp and Glu at Asn^{L27d}, Tyr^{L32}, and Tyr^{L92} of KD-247 may provide additional insights into the interactions with the GPGR V3 arch.

All scFv variants were expressed and purified by a stepwise refolding process (38) (Supplemental Fig. 1A) that overcomes the previously reported challenge of obtaining anti-V3 loop scFvs (64). Despite the low recovery of refolded monomeric scFvs, we were able to obtain sufficient quantities for the subsequent analyses. A correctly folded scFv should retain an immunoglobulin-like

structure with each variable domain consisting of nine antiparallel β-sheets (65). We previously used CD spectroscopy to confirm efficient refolding of WT KD-247 scFv (38). Here, we used far-UV CD spectroscopy to analyze the folding of mutant KD-247 scFv variants (Supplemental Fig. 1B–E). Protein folding can be assessed from the CD ellipticity value (y axis intercept): unordered protein structure increases with decreasing ellipticity value at short wavelength (200 nm) (66). Overall, the scFvs were better folded in the presence of a 16mer HIV-1$_{\mathrm{MN}}$-derived V3 peptide (Supplemental Fig. 1B–E; cf. right vs. left panels). Folding was further confirmed by analyzing the CD data using the SELCON3 (39, 40) and K2D3 (41) methods in the DichroWeb online analysis software (data not shown) (42, 43). Generally, the quantification of the CD data by SELCON3 and K2D3 confirm that the secondary structure of the Asn^{L27d} scFv variants had a comparable β-sheet content to that of WT scFv (Supplemental Fig. 1B). Of the Tyr^{L92} variants, results from the K2D3 method demonstrated that Phe^{L92}, Gln^{L92}, and Arg^{L92} showed the most comparable β-sheet content to WT scFv, which is again consistent with the CD spectra (Supplemental Fig. 1B). The results from the SELCON3 and K2D3 methods showed that Tyr^{L32} variants and the double mutants Y32A/Y92A and N27dA/Y32A exhibited lower β-sheet contents compared with WT scFv, which demonstrates poor folding in agreement with the CD spectra (Supplemental Fig. 1D, E). This observation indicated that the Tyr^{L32} aromatic ring is required for proper conformation of KD-247 when purified in vitro. We selected scFv variants

— 70 —

that showed a proper β-sheet profile for further investigation of the KD-247 scFv-V3 loop interactions.

scFv–V3 loop interactions

To compare binding of KD-247 scFv variants to GPGR V3 loop peptides, we performed a protein–protein interaction assay using the AlphaScreen technology (67). The streptavidin-coated donor beads and the nickel-chelate acceptor beads bind to the biotinylated V3 peptides and the purified His_6-tagged scFvs, respectively. A favorable interaction between the V3 loop peptide and the scFv variant brings the 2 types of fluorophore-coated beads into proximity, and an amplified light signal is generated upon excitation (Fig. 3A). Our results showed that similar to WT scFv, several scFv variants, including N27dD, N27dE, N27dK, N27dR, Y92A, Y92F, Y92R, and Y32F, interact with the clade B V3 loop peptide, and the signals measured were significantly different from the no-scFv negative control (Fig. 3B).

In addition to measuring the binding interactions of scFv with cyclic V3 loop peptides, we also determined their ability to neutralize the infectivity of pseudotyped

HIV-1 (HIV-1$_{JR-FL}$, Table 2) that contains a V3 loop similar to the one used in the modeling studies (HIV-1$_{MN}$-derived RP142 peptide). Only WT KD-247 Fab and scFv, as well as N27dD and Y92F scFvs, could neutralize by at least 80% pseudotyped clade B HIV-1 using 5 μM scFv (Fig. 3C). Other scFv variants, which initially showed binding to the clade B GPGR V3 loop peptide (Fig. 3B), neutralized less than 30% of pseudotyped HIV-1 under the same conditions (Fig. 3C).

We also determined the EC$_{50}$ of the most potent scFvs in TZM-bl neutralization assays using fully infectious CCR5-tropic HIV-1$_{BaL}$ and CXCR4-tropic HIV-1$_{MN}$ (Table 3). Similarly, the refolded WT scFv neutralized the replication-competent HIV-1$_{MN}$ and HIV-1$_{BaL}$ at comparable EC$_{50}$ values (0.7 and 0.6 μM, respectively). Y92F scFv showed similar EC$_{50}$ values compared to WT scFv (0.8 μM for HIV-1$_{MN}$ and 0.5 μM for HIV-1$_{BaL}$), suggesting that the aromatic interaction with this residue is crucial. A slight increase in the EC$_{50}$ of N27dD scFv (2.1 μM for HIV-1$_{MN}$ and 1.2 μM for HIV-1$_{BaL}$), indicated that Asn^{L27d} is better at stabilizing the interaction with Arg^{315}. These results provided insights into the interactions of Arg^{315} with side chains at the interface of the KD-247 light chain.
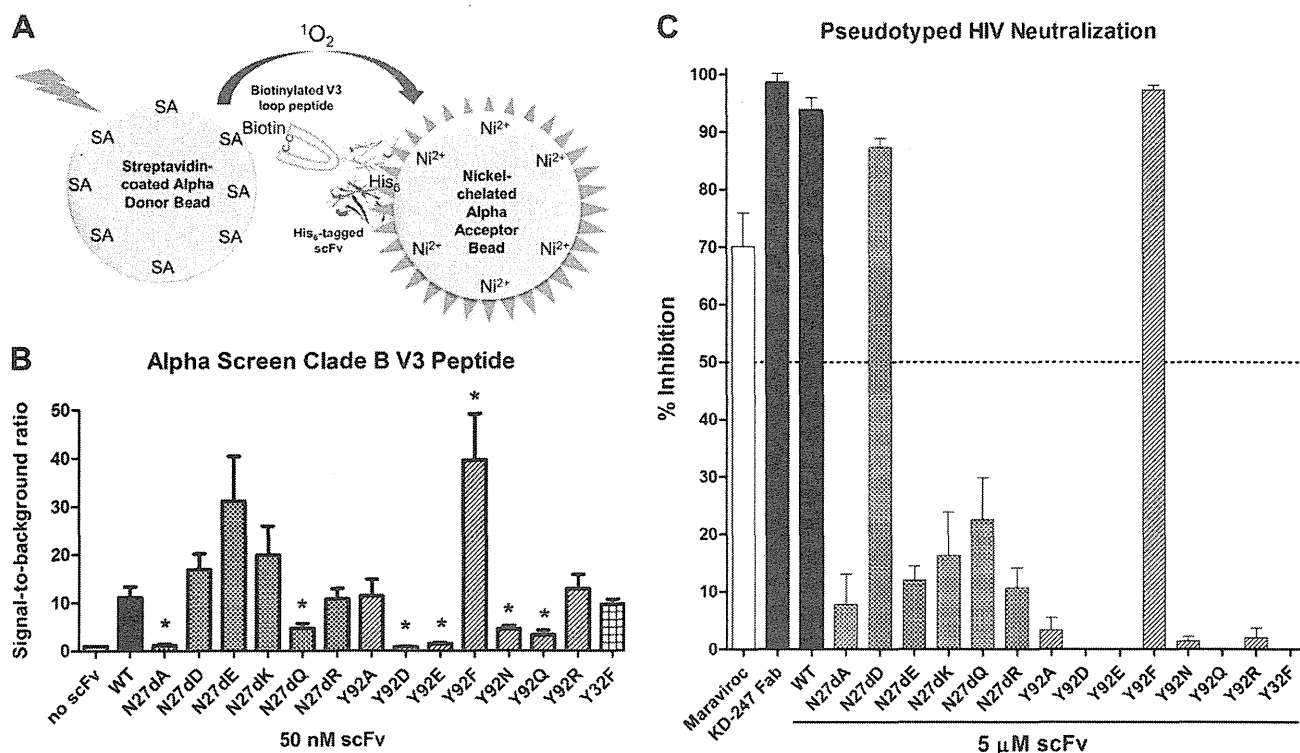

Figure 3. Interactions of scFv variants with V3 loop. (A) Schematic representation of KD-247 scFv interactions with a V3 peptide using AlphaScreen technology. His-tagged scFvs were allowed to interact with biotinylated V3 peptide. The interaction was detected using nickel (Ni^{2+})-chelated AlphaScreen acceptor beads and streptavidin (SA)-coated AlphaScreen donor beads. (B) Interaction of scFv variants with cyclic clade B V3 peptide. Results are expressed as the means of signal-to-background ratio from 3 independent experiments. Error bars indicate SEM. Statistically significant differences compared to WT scFv are represented by an asterisk (*$P < 0.05$). (C) Neutralization assay of HIV-1 Env pseudotyped virus on TZM-bl cells. A total of 10 nM maraviroc (CCR5 antagonist) or 5 μM KD-247 Fab or His-tagged scFv variants were preincubated with HIV-1$_{JR-FL}$ Env pseudotyped HIV-1 before infection of TZM-bl. Luminescence was measured 48 h after infection to determine scFv variants that result in >50% neutralization of pseudotyped virus. Results are represented as the average of percentage neutralization relative to virus control from at least three experiments; error bars indicate SEM.

TABLE 2. *V3 loop sequences of clade B HIV-1 strains*

HIV-1 strain	Tropism	V3 loop sequence
MN	X4	CTRPNYNKRKRIHIGPGRAFYTTKNIKGTIRQAHC
BaL	R5	-----N-T--S---------L---GE-I-D------
JR-FL	R5	-----N-T--S------------GE-I-D------

Dashes indicate identical amino acid residue.

DISCUSSION

The V3 loop of HIV-1 gp120 is flexible and structurally diverse, as evidenced by the wide range of different conformations of Arg[315] observed in gp120 and Fab/V3 complexes (aligned GPGR arches shown in Fig. 4A). This diverse loop, and specifically Arg[315], which correlates with genotypic specificity, is also recognized in a variety of ways by anti-V3 mAbs. Although most mAbs interact with their respective antigen through heavy chain interactions (68), several anti-V3 mAbs interact with Arg[315] through residues of their light chains. For example, murine Fab 83.1 interacts with Arg[315] through hydrogen bond between the main and side chains of Thr[L91] (55) (Fig. 4B). Human Fab 2219 recognizes Arg[315] through a hydrogen bond with Asn[L31] (69) (Fig. 4C). In the human F425-B4e8 Fab/V3 complex, Arg[315] is sandwiched between residues Tyr[L32] and Asp[L92] and is stabilized by a salt bridge with Asp[L92], as well as hydrogen bonds with the main and side chains of Asp[L92] (58) (Fig. 4D). Additionally, Arg[315] interacts with the human 1006-15D Fab through hydrogen bonds with the side chains of Asn[L30] and Asp[L93] (60) (Fig. 4E). KD-247 also uses its light chain to recognize Arg[315], but in what appears to be a different manner than other anti-V3 mAbs: in addition to hydrogen bond interactions with Tyr[L92] and van der Waals interactions with Tyr[L32] and Tyr[L92], Asn[L27d] also forms a hydrogen bond with the Arg[315] side chain, providing additional stability. Asn[L27d] and Tyr[L32] are held in place by an elaborate hydrogen bond network also involving Asp[L28] (Fig. 2D). These distinct interactions involve the unique CDR L1 insertion of KD-247 and provide a plausible answer for why Arg[315] is needed for HIV-1 neutralization by KD-247.

The interactions between mAbs and the V3 loop are also affected by the use of different CDRs. For example, the human mAb 537-10D recognizes the same IGPGR epitope as KD-247, yet it uses a long insertion in the CDR H3 loop to make nonspecific interactions with the V3 loop in the form of a 4-stranded antiparallel β-sheet

TABLE 3. *Fifty percent neutralization concentration (EC$_{50}$) (μM) against clade B HIV-1*

Assay	HIV-1$_{MN}$(CXCR4-tropic)	HIV-1$_{BaL}$(CCR5-tropic)
Maraviroc	>0.1	0.002 ± 0.001
KD-247 Fab	0.2 ± 0.06	0.1 ± 0.02
KD-247 scFv	0.7 ± 0.2	0.6 ± 0.1
N27dD scFv	2.1 ± 0.7	1.2 ± 0.2
Y92F scFv	0.8 ± 0.08	0.5 ± 0.09

Data represent the mean ± SD from the results of three independent experiments.

(Fig. 5A), in comparison to KD-247, which primarily uses CDR L1 for V3 loop interactions (Fig. 5B, C). Although they recognize the same epitope, 537-10D demonstrates a narrow HIV-1 neutralization profile
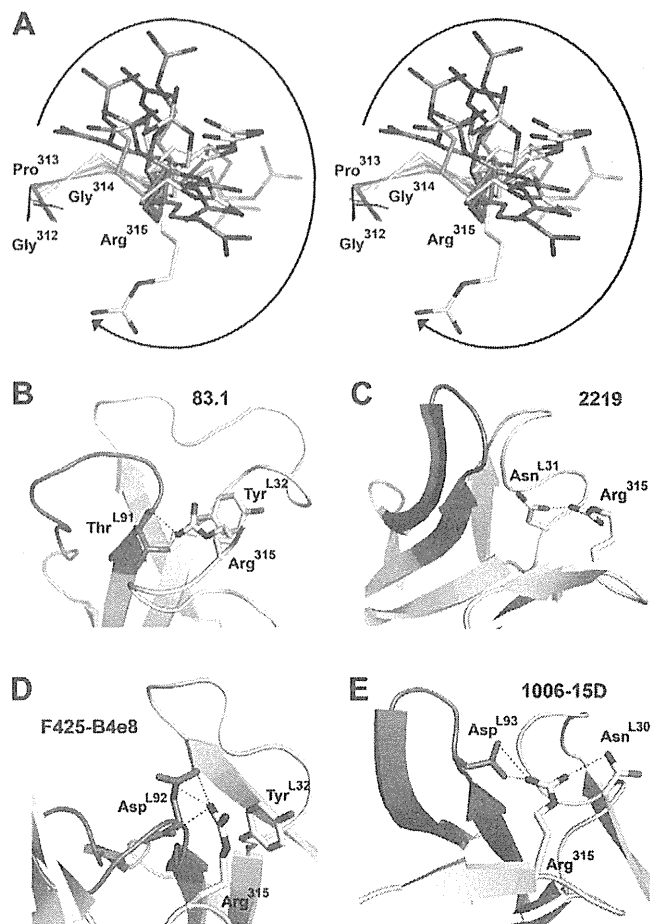

Figure 4. Structural variability of Arg[315] and recognition by anti-V3 mAb light chains. (A) Stereo view of "GPGR"-containing V3 loops in the following: 58.2 Fab complexes (PDB ID: 1F58, red; 2F58, green; 3F58, magenta), 83.1 Fab complex (1NAK, yellow); 447-52D (1Q1J, orange); 2219 Fab complex (2B0S, pink); F425-B4e8 Fab complex (2QSC, dark gray); 268-D Fab complex (3GO1, gray); 1006-15D Fab complex (3MLW, brown); 3074 Fab complex (3MLX, blue); 2557 Fab complexes (3MLR, light green; 3MLT, cyan); 2558 Fab complex (3UJI, mauve); 537-10D Fab complex (3GHE, hot pink); the V3 loop from the X5 Ab complex with JR-FL gp120 and CD4 (2B4C, dark green); and the V3 loop from the sulfated-tyrosine 412d Ab complex with YU2 gp120 and CD4 (2QAD, light blue). Arrow indicates the space occupied by Arg[315] conformations in the various structures. Arg[315] is also stabilized by interactions with light chain residues in some mAbs, including 83.1 (B), 2219 (C), F425-B4e8 (D), and 1006-15D (E). H bonds and salt bridges are shown as black and red dashed lines.
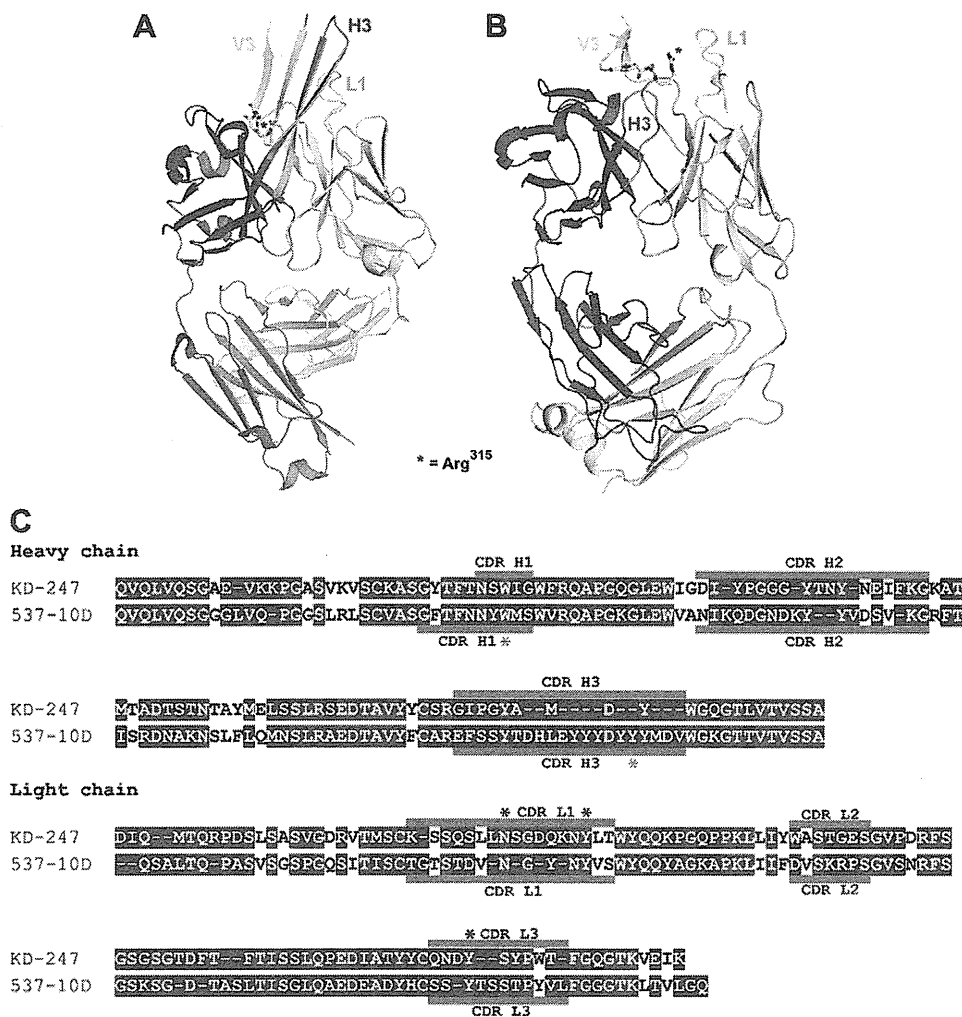
Figure 5. The 537-10D and KD-247 target the same IGPGR epitope using different modes of V3 binding. (A) 537-10D Fab (heavy and light chains in dark and light gray) in complex with an MN V3 peptide (yellow, PDB ID: 3GHE). The primary binding interactions occur in the CDR H3 loop (purple). (B) KD-247 Fab bound to the RP142 V3 peptide (same colors as in (A)). Most of the binding interactions occur in the CDR L1 loop (cyan). (C) Sequence alignment of the KD-247 and 537-10D variable regions (CDR regions in red). Identical residues are highlighted in blue and similar residues in yellow. Asterisks mark the residues making interactions with Arg^{315} of the RP142 V3 peptide. Sequence alignment was performed by the Sequence Manipulation Suite (*http://www.bioinformatics.org/sms2/index.html*). CDRs were labeled on the basis of previously published sequences (27, 59).

compared to KD-247 (70). This is likely due in part to the more restricted antigen binding site of 537-10D, in which the Trp^{H33}, Glu^{H95}, and Tyr^{H100J} residues that interact with Arg^{315} of the V3 loop are buried in a deep pocket (~6Å) that requires a close fit to bind the V3 loop. The CDR region of KD-247 demonstrates a shallow binding pocket that may be able to better tolerate flexibility of the V3 arch (59).

Resistance mutations at gp120 affect interactions between mAb and V3 loop and help HIV-1 escape neutralizing antibodies. Two mutations in the V3 arch region of gp120 cause resistance to KD-247. KD-247 neutralizes HIV-1$_{JR-FL}$ with a G314E mutation ~20-fold less efficiently than WT (62), and also binds 100× weaker than WT to HIV-1$_{BaL}$ with a V2 PNGS insertion in addition to the V3 R315K mutation (63). Our modeling studies suggest that mutation from Gly to Glu at 314 and from Arg to Lys at 315 creates steric interactions with the binding pocket of KD-247 (data not shown). These steric contacts likely affect KD-247 binding to V3 loops containing these mutations and may explain the reported differences in KD-247 binding and HIV-1 neutralization.

Our proposed interactions were validated by the generated scFv variants and the results of our binding and neutralization assays. The data suggest that KD-247 uses an elaborate network of interactions that are based on the long insertion in CDR L1 and involve residues Asn^{L27d}, Asp^{L28}, Tyr^{L32}, and Tyr^{L92} (Fig. 2D). Importantly, one of these residues (Tyr^{L32}) appears to be important for proper scFv folding, as almost all of the mutants at this position were inactive in neutralization assays (Fig. 3C) and poorly folded (CD spectra in Supplemental Fig. 1D). Phe^{L32} was the only mutant at position 32 that demonstrated proper scFv folding. Although variant Phe^{L32} demonstrated some binding activity to the V3 loop peptide (Fig. 3B), it did not neutralize pseudotyped clade B HIV-1 (Fig. 3C). Hence, an aromatic residue at position 32 in the light chain is important for proper scFv folding but not necessarily for neutralization, where it seems that the phenoxy group is critical. Changes at position 27d do not affect scFv folding (Supplemental Fig. 1B) and appear to either have limited effect (with the exception of Ala^{L27d} and Gln^{L27d}) or even enhance binding to the V3 loop (Fig. 3B). The loss of V3 loop binding and neutralization ability of the Ala^{L27d} KD-247 scFv variant is consistent with the proposed role of Asn^{L27} in interacting with Arg^{315}. However, the only variant that was able to efficiently neutralize pseudotyped clade B HIV-1 was Asp^{L27d} (Fig. 3C). It is likely that the Glu^{L27d} and Gln^{L27d} variants are not as efficient in neutralization of pseudotyped virus because of their longer side chains

(as compared to Asp^{L27d} and Asn^{L27d}). Similarly, the even longer side chains of Arg^{L27d} and Lys^{L27d} are likely to negatively affect interactions with Arg^{315} because of steric constraints. The ability of the N27dD variant to neutralize clade B HIV-1 suggests that KD-247 may be substituted with Asp^{L27d} to retain activity against clade B HIV. This substitution would still be able to participate in the intricate network of hydrogen bond interactions proposed in our model for recognition of Arg^{315}. Although many of the scFv variants at position 92 of the light chain demonstrated proper folding (Supplemental Fig. 1C), Phe^{L92} demonstrated enhanced binding to the clade B V3 loop peptide while Ala^{L92} and Arg^{L92} had similar binding compared to the WT scFv (Fig. 3B), but only Phe^{L92} showed effective neutralization of clade B HIV-1 Env pseudotyped virus (Fig. 3C). These results establish that the aromatic ring at Tyr^{L92} is essential for clade B V3 loop recognition. Overall, these observations highlight the importance of Asn^{L27d}, Tyr^{L32}, and Tyr^{L92} in neutralizing clade B HIV-1 containing a GPGR V3 loop arch. Importantly, these results reveal that binding of scFv variants to clade B V3 loop peptides does not necessarily correlate with efficient HIV-1 clade B neutralization. It is possible that other factors may affect binding of the antibody in the context of the full Env glycoprotein that do not factor in to V3 peptide binding. The recent crystal structure of the native Env trimer by Julien et $al.$ (71) revealed that the gp120 subunits are stabilized by β-hairpin interactions of the V3 loop and the V1/V2 strands B and C near the top of the trimer. The arch of the V3 loop is hidden by an N-acetyl glucosamine from the Asn^{197} glycan at the C-terminal region of V2 strand D from a neighboring protomer. This glycan blocks access to the V3 arch and may affect mAb binding.

Our findings are in agreement with previous work highlighting the dramatic flexibility of V3 loop and underscore the challenges in engineering antibodies that will be useful for treatment and vaccine design. Antibody engineering based on the interactions reported in our and other structures may lead to enhanced interactions with both Arg and Gln residues at position 315 of the V3 loop. For example, we expect that mutations of KD-247 residue Asn^{L27d} to longer polar residues (N27dQ, N27dK, and N27dR) should maintain the hydrogen bond interaction with clade B Arg^{315} and also be able to hydrogen bond with the shorter non–clade B Gln^{315}. Additionally, mutations of KD-247 residue Asp^{L28} to long polar residues (D28K, D28R, and D28E) should reach and interact with both clade B Arg^{315} and non–clade B Gln^{315}. Similarly, the Y32R mutant should maintain van der Waals interactions with clade B Arg^{315} and also make hydrogen bond interactions with non–clade B Gln^{315}. Combinations of the above mutations in the 27d, 28, 32, and 92 positions of the light chain of KD-247 may also help to maintain interactions with Arg^{315} and improve interactions with Gln^{315}. Additional approaches may include mutations of other KD-247 residues that do not interact directly with residue 315 of the V3 loop. Such interactions are observed in the structures of the 2557 and 3074 Fabs (22, 60) in complex with the V3 loop. Finally, extended CDR H3 loops may be designed to make nonspecific main chain interactions

with the V3 loop, as is the case with 447-52D (61) and 537-10D (59), which form three-stranded and four-stranded antiparallel β-sheets with the V3 loop target.

Although the propensity of V3 loop to serve as an immunogen to elicit broadly neutralizing antibodies against HIV-1 of multiple clades has been challenging, the extensive studies performed by the Zolla-Pazner, Gorny, Wilson, and Kong groups suggest that this strategy may be achievable (22, 25, 55, 58–61, 69, 70, 72). $\boxed{\text{FJ}}$

REFERENCES

1. Le Douce, V., Janossy, A., Hallay, H., Ali, S., Riclet, R., Rohr, O., and Schwartz, C. (2012) Achieving a cure for HIV infection: do we have reasons to be optimistic? *J. Antimicrob. Chemother.* **67**, 1063–1074

2. Wei, X., Decker, J. M., Wang, S., Hui, H., Kappes, J. C., Wu, X., Salazar-Gonzalez, J. F., Salazar, M. G., Kilby, J. M., Saag, M. S., Komarova, N. L., Nowak, M. A., Hahn, B. H., Kwong, P. D., and Shaw, G. M.(2003) Antibody neutralization and escape by HIV-1. *Nature* **422**, 307–312

3. Parren, P. W., Burton, D. R., and Sattentau, Q. J. (1997) HIV-1 antibody—debris or virion? *Nat. Med.* **3**, 366–367

4. Yusim, K., Korber, B. T. M., Brander, C., Barouch, D., de Boer, R., Haynes, B. F., Koup, R., Moore, J. P., Walker, B. D., and Watkins, D. I. (2011) HIV Molecular Immunology, Los Alamos National Laboratory, Theoretical Biology and Biophysics, Los Alamos, New Mexico, http://www.hiv.lanl.gov/content/immunology

5. Burton, D. R., Barbas III, C. F., Persson, M. A., Koenig, S., Chanock, R. M., and Lerner, R. A. (1991) A large array of human monoclonal antibodies to type 1 human immunodeficiency virus from combinatorial libraries of asymptomatic seropositive individuals. *Proc. Natl. Acad. Sci. USA* **88**, 10134–10137

6. Trkola, A., Purtscher, M., Muster, T., Ballaun, C., Buchacher, A., Sullivan, N., Srinivasan, K., Sodroski, J., Moore, J. P., and Katinger, H. (1996) Human monoclonal antibody 2G12 defines a distinctive neutralization epitope on the gp120 glycoprotein of human immunodeficiency virus type 1. *J. Virol.* **70**, 1100–1108

7. Stiegler, G., Kunert, R., Purtscher, M., Wolbank, S., Voglauer, R., Steindl, F., and Katinger, H. (2001) A potent cross-clade neutralizing human monoclonal antibody against a novel epitope on gp41 of human immunodeficiency virus type 1. *AIDS Res. Hum. Retroviruses* **17**, 1757–1765

8. Barbato, G., Bianchi, E., Ingallinella, P., Hurni, W. H., Miller, M. D., Ciliberto, G., Cortese, R., Bazzo, R., Shiver, J. W., and Pessi, A. (2003) Structural analysis of the epitope of the anti-HIV antibody 2F5 sheds light into its mechanism of neutralization and HIV fusion. *J. Mol. Biol.* **330**, 1101–1115